

ABSTRACT

A Novel Spectropolarimeter for Determination of Sucrose and Other Optically Active Samples

Carlos Enrique Calleja-Amador

Mentors: Kenneth W. Busch, Ph.D. and Marianna A. Busch, Ph.D.

Polarimetry and spectropolarimetry are important tools in the sugar industry and pharmaceutical research. Polarimetric measurements cannot be performed on colored samples because the presence of color interferes with the final reading. To avoid the effect of color in sugar samples, lead subacetate is added. Its use to decolorize sugar is problematic because lead is a pollutant. In this work, a novel spectropolarimeter based on an ordinary spectrophotometer is described for determination of sucrose and other optically active samples. The instrument has no moving parts, and optical rotation is encoded as apparent absorbance which makes it suitable for colored samples. Background correction before apparent absorbance measurements, combined with multivariate statistical analysis over a wide spectral range, proved efficient to avoid chemical pretreatment of the samples. The instrument showed good performance for sucrose predictions and multivariate enantiomeric discrimination.

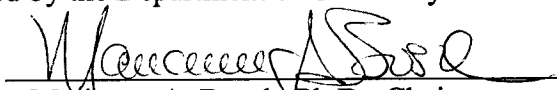
A Novel Spectropolarimeter for Determination of Sucrose
and Other Optically Active Samples

by

Carlos Enrique Calleja-Amador


A Thesis

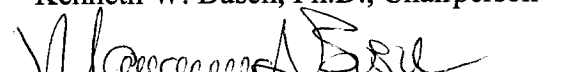
Approved by the Department of Chemistry and Biochemistry



Marianna A. Busch, Ph.D., Chairperson


Submitted to the Graduate Faculty of
Baylor University in Partial Fulfillment of the
Requirements for the Degree
of
Master of Science

Approved by the Thesis Committee


Kenneth W. Busch, Ph.D., Chairperson

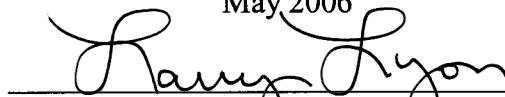

Marianna A. Busch, Ph.D., Chairperson


Stephen L. Gipson, Ph.D.


Charles M. Garner, Ph.D.


Marian M. Ortuno, Ph.D.

Accepted by the Graduate School
May 2006


J. Larry Lyon, Ph.D., Dean

Copyright © 2006 by Carlos Enrique Calleja-Amador

All rights reserved

TABLE OF CONTENTS

LIST OF FIGURES	v
LIST OF TABLES	ix
ACKNOWLEDGEMENTS.....	x
DEDICATION	xi
CHAPTER ONE	1
Introduction.....	1
<i>Polarized Light</i>	4
CHAPTER TWO	12
Polarimetry.....	12
<i>Polarimetry and Spectropolarimetry</i>	12
<i>Types of Molecules Analyzed by Polarimetry and/or Spectropolarimetry</i>	15
<i>The Sugar Industry</i>	16
<i>Polarimetric Measurements for Quality Assessment</i>	17
<i>Recent Methods for Sucrose Determination</i>	20
<i>Optical Activity Measurements in the Pharmaceutical Industry</i>	23
CHAPTER THREE	25
Theoretical Considerations	25
CHAPTER FOUR.....	31
Experimental Section	31
<i>Apparatus</i>	31
<i>Reagents</i>	33
<i>Sucrose Determinations</i>	33
<i>Enantiomeric Discrimination</i>	33
<i>Experimental Procedure</i>	33
CHAPTER FIVE	36
Results and Discussion	36
<i>Sucrose Determination</i>	36
<i>Enantiomeric Discrimination</i>	54
CHAPTER SIX.....	60
Conclusions.....	60

APPENDIX.....	62
Other Models Tested To Predict Sucrose Concentrations	63
Spectropolarimetric Determination of Sucrose Inversion Using	
Absorbance Measurements	68
Additional Results on Enantiomeric Discrimination	73
Spectropolarimetric Configuration	76
REFERENCES	77

LIST OF FIGURES

Figure	page
1. Schematic representation of the Glan-Thompson and Glan-Taylor polarizers. ..	1
2. a. Cartesian system showing the direction of propagation of a beam. b. Schematic representation of a transverse wave with its electric and magnetic vectors, propagating to the right.....	5
3. Multiple directions of oscillation of a transverse wave. a. A representation of the planes of oscillation. b. View representing the direction of propagation.	6
4. Production of linearly polarized light.	7
5. a. Diagonal view of orthogonal electric fields produced when linearly polarized light is incident on a polarizer. b. Electric fields with a 90° shift, as required to produce circularly polarized light.	8
6. a. Right circularly polarized light, corresponding to a phase shift of 90° . b. Left circularly polarized light with a phase shift of 270°	8
7. Schematic representation of the production of polarized light by reflection.....	9
8. Schematic representation of the production of polarized light by scattering.....	9
9. Production of polarized light by double refraction using birefringent materials, such as a Nicol prism.	10
10. Representation of the production of circularly polarized light from linearly polarized light using a retarding device.	11
11. Schematic representation of a conventional polarimeter.	12
12. Representation of the change in intensity of a beam crossing a set-up of a. two parallel polarizers and b. two perpendicular polarizers.	25
13. Set-up of two polarizers at a fixed angle of 45 degrees.	26
14. Ideal plot of change in absorbance as function of the optical activity.....	27
15. Schematic representation of the spectropolarimetric set-up.	31

16.	Expanded view of the sample holder arranged with a crossed polarizers set-up.....	34
17.	Fragment of the optical rotatory dispersion (ORD) curve of sucrose generated from the wavelengths of operation of a Rudolph Autopol III Polarimeter.....	36
18.	Fragment of an ORD spectrum –absorbance vs. wavelength- of sucrose, generated from the wavelengths of operation of a Rudolph Autopol III Polarimeter.....	37
19.	Absorbance vs. angle of rotation at the polarimetric wavelengths.....	38
20.	Angle of rotation vs. concentration as recorded polarimetrically.....	39
21.	Apparent absorbance vs. concentration. Plot generated using a crossed polarizers spectrophotometric set-up, at the polarimetric wavelengths.....	39
22.	Optical rotatory dispersion spectrum for 20% by mass in sucrose recorded using the new spectropolarimetric arrangement.....	40
23.	ORD-type curve for 5% w/w sucrose obtained using a novel polarized spectrophotometric set-up with a water blank.....	42
24.	ORD curve for 5% w/w sucrose obtained using a novel polarized spectrophotometric set-up with the same solution as a blank.....	42
25.	Calibration curve used for the determination of sucrose by polarimetry.....	44
26.	Multivariate regression model based on partial least squares, for a calibration set between 750 nm and 925 nm using water blank.....	46
27.	Multivariate regression model based on partial least squares, for a calibration set between 750 nm and 925 nm using background correction.....	48
28.	Colored sugar samples. From left to right: pure sucrose, raw sugar, light brown sugar, dark brown sugar and coffee.....	50
29.	Overlaid spectra of four colored samples of sugar using NIR spectropolarimetry.....	51
30.	Angle of rotation vs. time for the inversion of sucrose followed polarimetrically at 589 nm.....	52
31.	Absorbance vs. time for the inversion of sucrose followed spectropolarimetrically at 589 nm.....	52

32.	Absorbance vs. time for the inversion of dark brown sugar followed spectropolarimetrically at 850 nm.	53
33.	Optical rotatory dispersion for S and R limonene using an Autopol III Polarimeter between 350 and 650 nm.....	54
34.	Optical rotatory dispersion spectra for S and R limonene recorded using a set of crossed polarizers fixed at 45 degrees from one another.....	55
35.	PLS1 model used to predict %R in a mixture of enantiomers for limonene.	56
36.	PLS1 model used to predict %S in a mixture of enantiomers for limonene.....	58
37.	PLS1 model used to predict total concentration of limonene in a mixture of enantiomers.	59
A.1.	PLS1 model using 36 samples of colorless sucrose solutions between 750 and 950 nm.	66
A.2.	Model using water blank for 100 samples of colorless sucrose solutions between 282 and 372 nm.....	67
A.3.	Model with background correction for 100 samples of colorless sucrose solutions between 282 and 372 nm.....	68
A.4.	Model using water blank for 100 samples of colorless sucrose solutions between 500 and 700 nm.....	69
A.5.	Model with background correction for 100 samples of colorless sucrose solutions between 500 and 700 nm.....	69
A.6.	Model using background correction for light brown sugar solutions between 750 and 950 nm.	70
A.7.	MS-Excel worksheet to determine the rate constant by curve fitting using the solver tool.....	74
A.8.	a. MS-Excel solver parameters for curve fitting of inversion data, and b. solver options to assess curve fitting.....	75
A.9.	Overlaid plot of the experimental and fit data for sucrose inversion followed by absorbance measurements using a spectropolarimetric arrangement of fixed crossed polarizers.	76

A.10.	Optical rotatory dispersion for (<i>S,S</i>)-(-)- <i>N,N'</i> -bis(a-methylbenzyl)sulfamide and (<i>R,R</i>)-(+)- <i>N,N'</i> -bis(a-methylbenzyl)sulfamide using an Autopol III Polarimeter between 350 and 650 nm.....	76
A.11.	Optical rotatory dispersion for (<i>S,S</i>)-(-)- <i>N,N'</i> -bis(a-methylbenzyl)sulfamide and (<i>R,R</i>)-(+)- <i>N,N'</i> -bis(a-methylbenzyl)sulfamide using a set of crossed polarizers fixed at 45 degrees from one another.	77
A.12.	Optical rotatory dispersion for L-arabinose and D-arabinose using an Autopol III Polarimeter between 350 and 650 nm.....	77
A.13.	Optical rotatory dispersion for L-arabinose and D-arabinose using a set of crossed polarizers fixed at 45 degrees from one another.	78
A.14.	PLS1 model used to predict %R in a mixture of enantiomers for arabinose.	78
A.15.	Spectropolarimetric set-up used in this project.	79
A.16.	Relative position of the spectropolarimetric cell for: a. background correction, and b. ORD spectrum recording.	79

LIST OF TABLES

Table	page
1. Chart used to determine sucrose content from % Pol and Brix values.....	19
2. Sucrose concentrations expressed as % by mass of pure sucrose using three different methods.	45
3. Sucrose concentrations expressed as % w/w in colored samples using background correction between 750 nm and 925 nm.	49
4. Values of the rate constants obtained for one colorless sample and one colored sample, by conventional polarimetry and using spectropolarimetry with background correction, respectively.	53
5. Results of the prediction of enantiomeric composition expressed as % of (R)-(+)-limonene, using PLS1 between 450 and 750 nm.	57
6. Results of the prediction of enantiomeric composition expressed as % of (S)-(-)-limonene, using PLS1 between 450 and 750 nm.	58
7. Prediction of total concentration of limonene using PLS1 between 450 nm and 750 nm.....	59
A.1. Results obtained with the models shown in Figures A.2 and A.3.	68
A.2. Results obtained with the models shown in Figures A.4 and A.5.	70

ACKNOWLEDGMENTS

The author wants to acknowledge the following people who contribute to make this project possible: Dr. Kenneth W. Busch and Dr. Marianna A. Busch for their support and patience during the progress of this work. To Dr. Dennis Rabbe for his valuable contributions, as well as my lab mates in the Center for Analytical Spectroscopy: Christopher Davis, Jemima Ingle, Jody Harvey and Selorm Modzabi, for their patience and friendship during this time. To Dr. Kevin Pinney for his support allowing the use of the Autopol III Polarimeter in his research laboratory. Gratitude is also extensive to the Department of Chemistry and Biochemistry, and Baylor University for supporting this research and giving me the opportunity to be here.

A special acknowledgment is made to the authorities of the Direccion Tecnica de Servicios de Salud, Centro de Desarrollo Estrategico e Informacion en Salud y Seguridad Social, and Caja Costarricense de Seguro Social, for their support during this period. Also to my beloved Costa Rica, to which I hope I can give back as much as I have received.

I would also like to express my sincere gratitude to the people who made this time a wonderful experience in my life, for their friendship and permanent support, especially my mother Sonia Amador, and my friends Rigoberto Blanco, Francisco Gonzalez and Franklin Beckles who are an important part of this accomplishment.

To my wife Desiree and my daughter Jimena, with all my love.

CHAPTER ONE

Introduction

Polarized light waves are light waves in which the vibrations occur in one direction. The process of transforming unpolarized light into polarized light is known as polarization. There are two main types of polarization: linear and circular. Each of these types can be achieved using different devices.¹

The most common method to produce linear polarization involves the use of two calcite prisms pasted together. Available commercial types of calcite polarizers are the Glan-Thompson and the Glan-Taylor polarizers. In the Glan-Thompson configuration the two halves are cemented together with Canada balsam. In the Glan-Taylor type, the two halves are separated by an air space, as shown in Figure 1.^{2, 3}

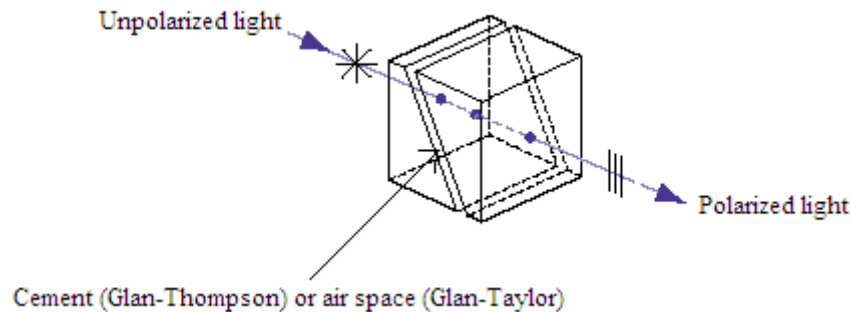


Figure 1. Schematic representation of the Glan-Thompson and Glan-Taylor polarizers.

Circular polarization is produced from linearly polarized light. Linearly polarized light is the result of the coherent superposition of two circularly polarized beams, a right and a left one. When light is passed through a polarizer, the resultant beam is linearly polarized.⁴ If a phase shift of 90° is induced in this linearly oscillating component using a device called a quarter-wave plate, then circularly polarized light is produced. If the quarter-wave plate is substituted by a photoelastic modulator, left-and right-circularly polarized light can be produced alternately.

Both linearly polarized and circularly polarized light have important chemical applications. The latter is used in techniques such as circular dichroism, and most recently vibrational circular dichroism (VCD). VCD has emerged as a powerful tool in the study of enantiomeric composition, determining the absolute configuration of chiral molecules, or observing the dynamics of proteins in aqueous solution, among others.¹

Linearly polarized light has been traditionally associated with polarimetry and the optical activity of molecules based on the Law of Malus, which states that the intensity of light varies according to $I = \cos^2 \beta$, where I is the intensity of light and β is the angle between the polarizers in a polarimeter. Optical activity is determined by measuring the angle of rotation of the plane of polarization of light. In the past, polarimetric measurements were done at a single wavelength; however, with the availability of modern instruments it is possible to determine the variation in angle of rotation in a range of wavelengths. The instrument used to perform these measurements is called a spectropolarimeter. A plot of angle of rotation against wavelength is known as an optical rotatory dispersion curve, and can provide important structural information, especially if the molecules do not have chromophores.⁵

Polarimetry remains as an important tool in the sugar industry and in pharmaceutical research, mostly for quality assurance purposes. In the sugar industry polarimetry is referred to as saccharimetry. Saccharimetric measurements are performed with a saccharimeter, which is a polarimeter calibrated to give directly the concentration of sucrose in a sample, or is used to determine the percentage of invert sugar. Invert sugar is the general name given to the disaccharide sucrose after being hydrolyzed to the monosaccharides glucose and fructose. The presence of invert sugar is important because it is an indicator of sweetness.⁶

Sucrose is obtained from two main sources: sugar cane and beets. In either case, saccharimetric measurements cannot be performed on colored samples because the presence of color reduces appreciably the intensity of light passing through the saccharimeter, interfering with the final reading of the instrument. To avoid the effect of colored solutions, lead subacetate is added as a decolorizer.⁶ Use of lead subacetate to decolorize sugar samples has become increasingly problematic because it is a pollutant difficult and expensive to dispose of. Some clarification methods have been proposed for the sugar industry, which use aluminum salts as clarifying agents. Others have proposed the use of near-infrared techniques to avoid color interferences and chemical pretreatment.^{7, 8}

In this work, a novel spectropolarimetric set-up, based on an ordinary spectrophotometer, will be evaluated for the determination of sucrose. The instrument allows the combination of spectrophotometric measurements with multivariate statistical analysis over a wide spectral range, and offers several potential advantages over

conventional polarimetry and spectropolarimetry. Additionally, this instrument will be tested as a device for enantiomeric determination, increasing its range of applicability.

The objectives of this work are:

1. To describe a novel spectropolarimeter for sucrose determination and enantiomeric discrimination;
2. To explain how measurements done with this instrument are equivalent to those performed with a conventional polarimeter or spectropolarimeter in agreement with the Law of Malus;
3. To show that the generated spectra are equivalent to an optical rotatory dispersion curve;
4. To use the device for sucrose determination;
5. To develop a model for sucrose determination based on multivariate regression techniques;
6. To present a methodology for background correction and its applicability to colored samples to avoid the need for clarifying agents in sucrose determinations;
7. To compare the rate constants for sucrose inversion obtained with polarimetry and with the proposed spectropolarimeter;
8. To use the instrument for enantiomeric discrimination of chiral molecules of pharmaceutical interest; and
9. To compare the results with those obtained with conventional polarimetry in enantiomeric discrimination.

In order to have a better understanding of the proposed spectropolarimetric arrangement, some properties of polarized light are described in the following section.

Polarized Light

Light has a dual character. It can behave as a particle as well as a wave. When viewed as a wave, light has two main components: an electric and a magnetic vector. These two kinds of vectors oscillate perpendicularly to each other. When such a wave

propagates in a direction perpendicular to both sets of components, it is called a transverse wave.⁴ In Figure 2a, the y axis represents the electric vector, the z axis the magnetic vector, and the x axis the direction of propagation. Figure 2b represents the nature of a transverse wave, where the electric vector oscillates in the same plane that contains the axis of propagation. Because a light wave does not have just one axis of oscillation for the electric and magnetic vector, there are an infinite set of possible orientations as shown in Figure 3.

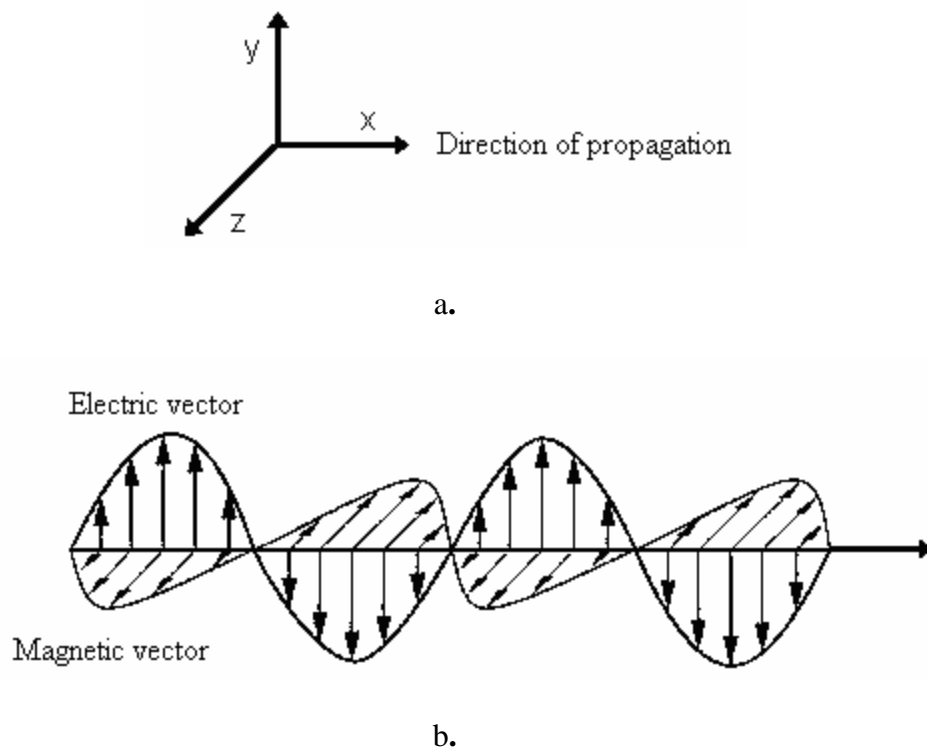


Figure 2. a. Cartesian system showing the direction of propagation of a beam. b. Schematic representation of a transverse wave with its electric and magnetic vectors, propagating to the right.

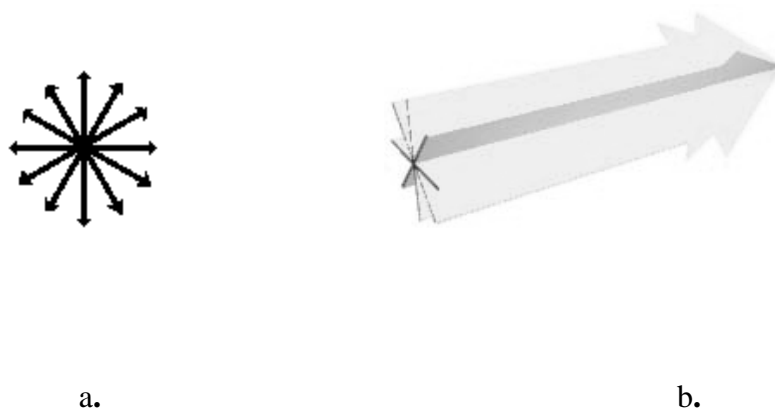


Figure 3. Multiple directions of oscillation of a transverse wave. a. A representation of the planes of oscillation. b. View representing the direction of propagation.

When a beam contains all possible components of its oscillating vectors, it is called unpolarized light. An example of unpolarized light is sunlight. However, if some of these oscillating vectors are filtered from the original beam, light is said to be polarized. This can be achieved using filtering devices such as prisms, reflective surfaces or absorbing materials (called dichroic materials), which act as polarizers. The type of polarizer used determines the kind of polarization produced: linear or circular. Circular polarization is a specific case of a more general form called elliptical polarization.⁴

With unpolarized radiation, an electromagnetic wave traveling towards an observer will show more than one plane of vibration for the electric (and magnetic) vector(s), as is represented in Figures 2 and 3. When light passes through a polarizing filter, the electric and magnetic fields are restricted to a single plane of oscillation. The wave is said to be plane polarized or linearly polarized. Polarization is a phenomenon exhibited only by transverse waves.⁴

For a clearer understanding, the wave model can be simplified by considering only the electric field. When light is passed through a polarizing filter (like a prism), all vectors are absorbed by the filter except one. This non-absorbed component continues to

vibrate in a single plane.¹ Figure 4 shows a schematic view of a transverse wave passing through a filter to produce linearly polarized light. Once it has passed the filter, the remaining electric vector oscillates in one plane.

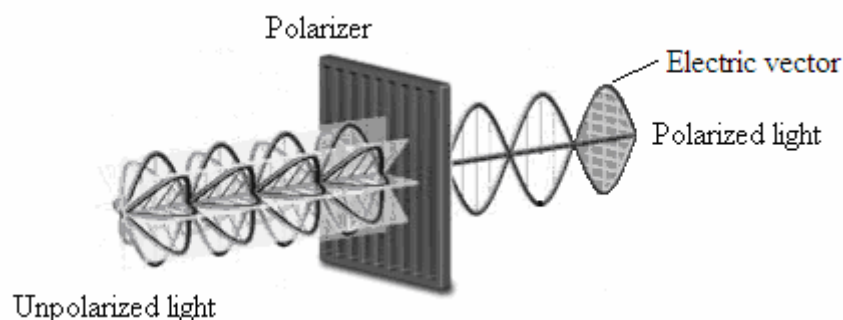


Figure 4. Production of linearly polarized light.

Circular polarization can be produced from linearly polarized light since the latter can be visualized as the coherent superposition of two circularly polarized beams rotating in appropriate directions at the same frequency. Figure 2b showed how the amplitudes of the electric vectors of light are in phase in a linearly polarized beam. When these amplitudes are of equal magnitude, but shifted 90° from one another, circularly polarized light is produced.⁹ Figure 5a shows a diagonal view of Figure 2b. Figure 5b shows the 90° displacement. The phase of this shift ($\pm 90^\circ$) makes circularly polarized light to oscillate either as right or left circularly polarized radiation.

If a wave of the same shape as that in Figure 5b were approaching an observer, the electric vectors would appear to be rotating to the right, and it would be right-circularly polarized light (Figure 6a). If it rotates to the left, then it will be left-circularly polarized

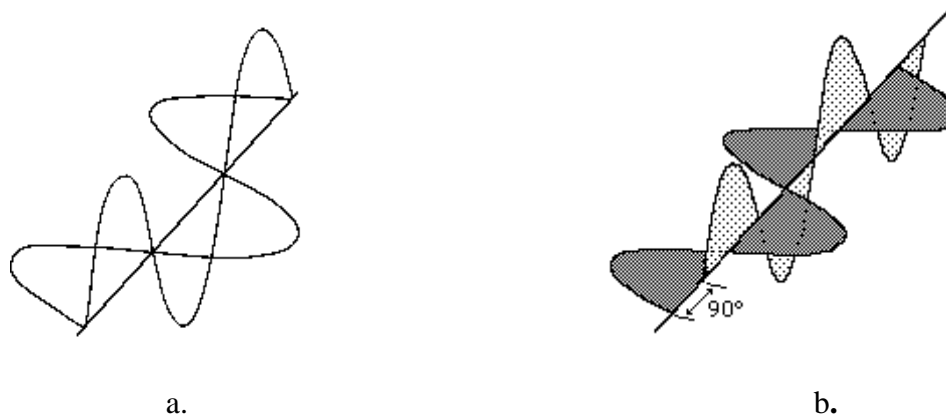


Figure 5. a. Diagonal view of orthogonal electric fields produced when linearly polarized light is incident on a polarizer. b. Electric fields with a 90° shift, as required to produce circularly polarized light.

light. The electric field vector completes one cycle of rotation as the light advances one wavelength towards the observer (Figure 6b). There is a phase difference of 180° between the right (Figure 6.a.) and left (Figure 6.b.) circularly polarized light. If the amplitudes of the electric vectors are not equal, elliptically polarized light is produced.⁹

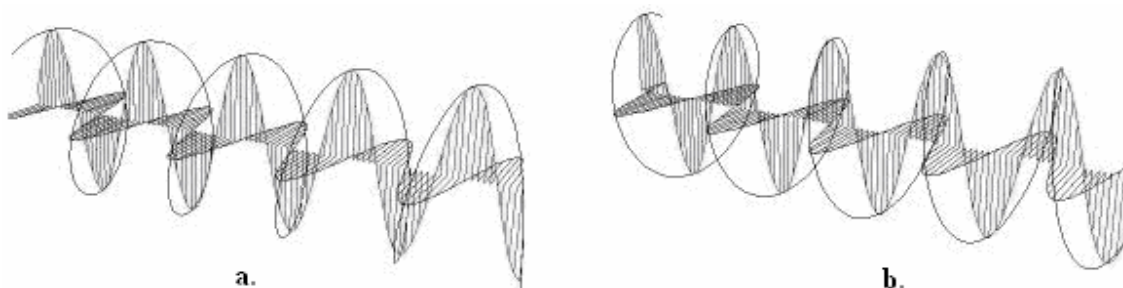


Figure 6. a. Right circularly polarized light, corresponding to a phase shift of 90° . b. Left circularly polarized light with a phase shift of 270° .

There are three main ways to produce polarized light: reflection, scattering and birefringence or double refraction. The first technique takes advantage of the reflective properties of nonmetallic materials. Figure 7 shows how polarized light can be produced by reflection. Light reflected from the surface is 100% polarized in the plane orthogonal to the plane of incidence.⁴

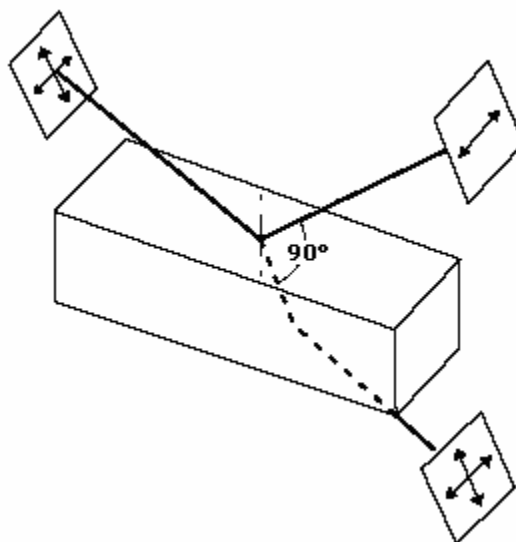


Figure 7. Schematic representation of the production of polarized light by reflection.

Figure 8 shows how polarized light can be produced by scattering. In scattering, light interacts with a filter that consists of molecules acting as dipole radiators. Since light is a transverse wave, the scattered component must be oriented at right angles to the direction of propagation.

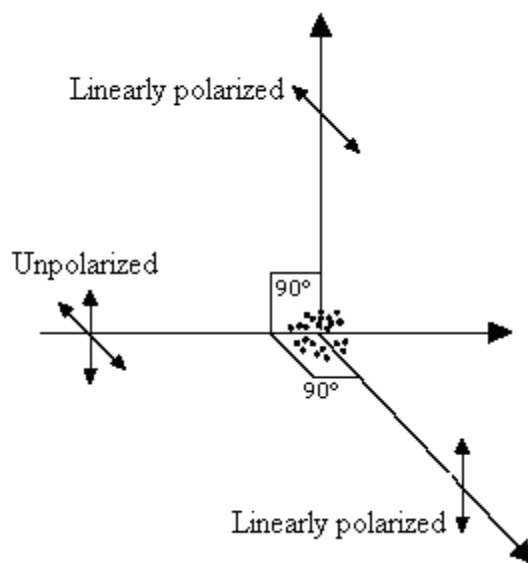


Figure 8. Schematic representation of the production of polarized light by scattering.

Birefringent materials divide an incoming beam in two rays. The phenomenon is known as birefringence, or double refraction, and it appears when light passes through a filter set up where it exhibits different indices of refraction. Filters can be designed to eliminate specific planes of vibration in the light, leaving those for the production of polarized light,^{2,10} as shown in Figure 9.

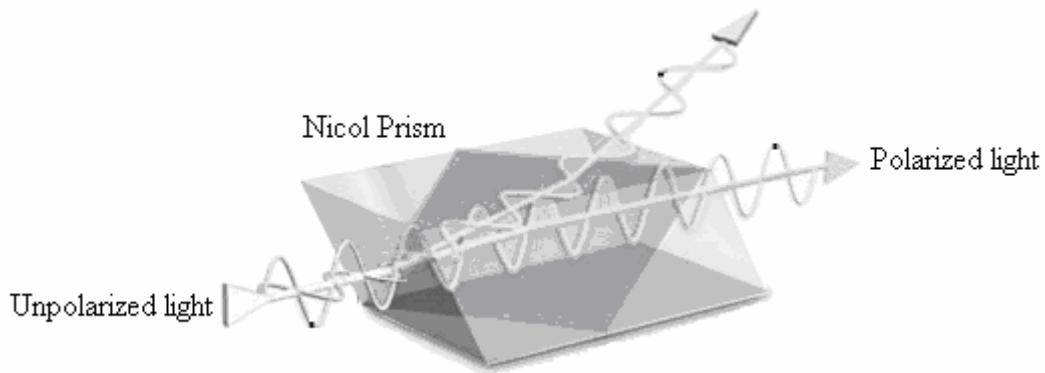


Figure 9. Production of polarized light by double refraction using birefringent materials, such as a Nicol prism.

Glan-Thompson and Glan-Taylor polarizers are more common birefringent devices because of their wider spectral range. Both are made of calcite, which is a naturally occurring birefringent crystal, and are useful from 250 to 2500 nm. The incident unpolarized beam is decomposed into two orthogonal polarization states called principal polarizations.³ Principal polarizations that travel at the same velocity through the first half of the polarizer (Figure 1) define the optic axis of the prism. When the principal polarizations pass the first half, they pass through a second refractive medium: a refractive cement in Glan-Thompson polarizers, or air in the Glan-Taylor polarizers, as was shown in Figure 1. Polarizations that have different velocities, have different indexes of refraction in the first half of the polarizer. These polarizations are reflected at

different angles from the optic axis by the second half. In a Glan-Thompson polarizer the optic axis usually has a tolerance of 15° . Glan-Taylor polarizers have an optic axis with a tolerance of 8° .^{2,3}

Circular polarization is usually obtained from a linearly polarized beam using a photoelastic modulator or a quarter wave plate to retard the phase of the wave. Both devices produce the 90° phase shift necessary to generate circular polarization. A quarter-wave plate induces a static phase shift,⁹ while a photoelastic modulator produces right-and left-circularly polarized beams can be produced at alternating intervals. This is the basis of modern circular dichroism spectrometers, which measure the difference in absorption, between left-and right-circularly polarized radiation.¹ Figure 10 shows how circular polarization is produced from a linearly polarized beam using both devices.

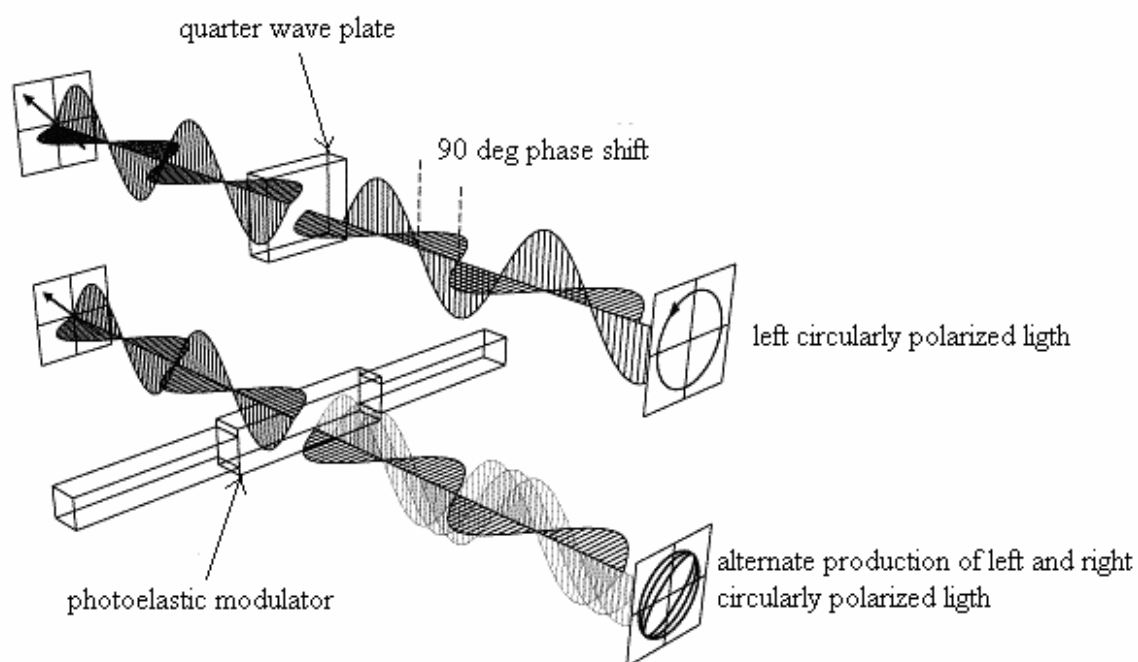


Figure 10. Representation of the production of circularly polarized light from linearly polarized light using a retarding device.

CHAPTER TWO

Polarimetry

Polarimetry and Spectropolarimetry

Conventional polarimeters consist of a monochromatic light source emitting radiation at 589 nm, a polarizer, a sample cell, an analyzer (which is a second polarizer) and a light detector, as shown in Figure 11. When unpolarized light passes through the polarizer, it becomes linearly polarized and its oscillation is restricted to a plane defined by the orientation of the polarizer. As it reaches the analyzer, the intensity of light passing out of the assembly will vary as the analyzer is rotated about its axis. When the planes of the two polarizers are coincident, the light intensity that passes through the combination will be at a maximum. When the planes of the two polarizers are at 90° , the light intensity will be at a minimum.⁵

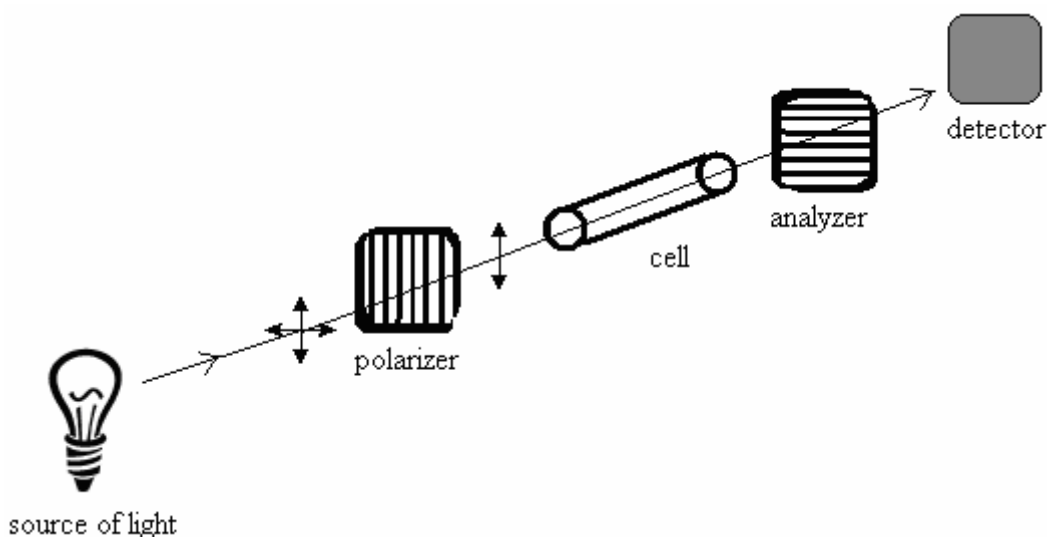


Figure 11. Schematic representation of a conventional polarimeter.

Polarimeters are usually arranged so that the two polarizers are at 90° to one another. Under this arrangement, no light should pass through the second polarizer. This is called the null condition. If an optically active sample is placed between the two polarizers, it will rotate the plane of polarized light so that some light passes through the analyzer. If the analyzer is rotated so that the light is once again extinguished, the angle by which the polarizer was rotated is the optical activity of that sample.¹¹ The amount of rotation caused by a given sample is proportional to the concentration of the sample, and the path length of the cell used as shown in Equation 2.1, where $[\alpha]$ is the specific rotation of the molecule, T is the temperature, λ the wavelength of the source, α is the measured angle of rotation, c the concentration in g/100 mL and l is the length of the polarimetric cell.⁵

$$[\alpha]_{\lambda}^T = (\alpha_{\lambda}^T)/c \cdot l \quad (2.1)$$

The determination of optical rotation can be accomplished rotating the analyzer manually or by electronic modulation at just one wavelength,⁵ or in a range of wavelengths. Simple polarimeters work at 589 nm. More sophisticated instruments, called spectropolarimeters work in a range of wavelengths.⁵ A spectropolarimeter is useful to study the variation of optical rotation with wavelength. This generates a special kind of curve called an optical rotatory dispersion curve, or ORD.¹

The possibility of recording ORD curves is useful in an increasing number of fields of research in organic chemistry and biochemistry. Many natural products are optically active. Their presence in living tissues and fluids can be studied and confirmed by measuring the wavelength at which maximum rotation occurs. The degree of rotation is especially useful when no chromophores are present, or in the presence of compounds

that absorb strongly in some region of the spectrum but are not optically active.⁵

Modern polarimeters and spectropolarimeters are more sensitive, and have become a reliable means to measure low concentrations of optically active substances. They have several novel applications in the pharmaceutical and food industries, and are used in a single wavelength mode (conventional polarimetry), in a range of wavelengths (spectropolarimetry), and in chiral HPLC coupled with UV-visible detection.¹²

Polarimetric and spectropolarimetric measurements involve four factors for the optimum performance of the instrument, either by itself or as a chromatographic detector: a) stability of the source, b) quality and extinction coefficient of the polarizers, c) the effect of modulation frequency for instruments that use some kind of modulation, and d) whether a design with modulation is superior to one without modulation.¹³ The dominant source of noise in a polarimeter is that from the light source. This occurs because, even though the light source noise is constant, it does not continue to be constant as it passes through the polarizers, and increases if polarization modulation is employed.¹³

A complete discussion of the performance of modern polarimeters was presented by Voigtman.¹³ Based on computational modeling of an ideal polarimeter, he was able to determine the effect of different components of the instrument on its sensitivity. Such modelling involved obtaining hypothetical detection limits while changing the source noise, the frequency of modulation and using polarizers with different extinction coefficients. In previous work, Yeung and coworkers concluded that high quality polarizers are important to increase signal-to-noise ratio. In their study, these workers reported a detection limit of 2.7×10^{-7} degrees.¹³ Yeung's work was based on the

analysis made by Kankare and Stephens, who reported a detection limit of 3×10^{-4} degrees.¹³ These works studied polarimetric and spectropolarimetric devices that used Faraday modulation, which is the most used mechanism to rotate electronically the analyzer. Faraday modulation is based on the Faraday effect, which is the rotation of the plane of polarization of polarized light in a magnetic field. When an optically active sample interacts with polarized light, the null condition is reached automatically when the effect of an electromagnetic field on the polarized beam is converted into mechanical rotation of the analyzer prism. No study has been made yet on a spectropolarimeter with no moving parts that might not require any modulation at all, which is proposed in the present work.

Types of Molecules Analyzed by Polarimetry and/or Spectropolarimetry

For a molecule to be analyzed using polarimetry, it should be optically active. Optical activity is a consequence of chirality. The most common types of optically active molecules are those with an asymmetrical carbon (a carbon attached to four different groups). This kind of substances occur in pairs of enantiomers, which are mirror-image isomers that have identical chemical and physical properties, making them difficult to separate and quantify.⁵ Polarimetry is particularly important in the sugar industry. Sucrose is optically active, and its concentration in extracts can be rapidly determined by measuring the degree of rotation of light after it has passed through the sample.⁵ Another important application of polarimetry is in the pharmaceutical industry. Many drugs are optically active. However, the physiological activity may depend on the particular enantiomer administered. Therefore enantiomeric discrimination is important in

increasing the efficacy of drugs, and more recently in environmental monitoring of unmetabolized residues once they have been excreted from the body.^{5, 14}

The Sugar Industry

Commercial sugar is produced from sugar cane and beets. Sugar cane processing is focused on the production of commercial sugar (sucrose), and invert sugar. In the United States, sugar cane is produced, harvested, and processed in four states: Florida, Louisiana, Texas, and Hawaii. The process of production involves several steps. The cane is received at the mill and prepared for extraction of the juice. The milling process involves breaking the hard structure of the cane, grinding the cane, and imbibition, to enhance the extraction.. The juice from the mills is strained and then clarified.¹⁵

In raw sugar production, clarification is done almost exclusively with heat and lime (as milk of lime or lime saccharate); small quantities of soluble phosphate also may be added. Lime is added to neutralize the organic acids, and the temperature of the juice is raised to about 95°C (200°F). A heavy precipitate forms which is separated by gravity from the juice in a clarifying tank.¹⁵ Evaporation follows filtration and is performed in two stages: initially in an evaporator station to concentrate the juice, and then in vacuum pans to crystallize the sugar. The evaporator station in cane sugar manufacture typically produces syrup with about 65 % solids and 35 % water.¹⁵ After evaporation, the syrup is clarified by adding lime, phosphoric acid, and a polymer flocculent, aerated, and filtered in the clarifier. From the clarifier, the syrup goes to the vacuum pans for crystallization, where a mixture of liquor and crystals known as massecuite is produced.¹⁵ The massecuite is then separated by centrifugation into the mother liquor (molasses) and the

sugar crystals. This process is repeated three more times, yielding highly pure sucrose from the first two separations, and black strap molasses for cattle feed in the third.¹⁵

The production of sugar from beets is less time consuming than that for sugar cane production. The processing starts by slicing the beets into thin chips. This process increases the surface area of the beet to make it easier to extract the sugar. The extraction takes place in a diffuser where the beet is kept in contact with hot water for about an hour. The exhausted beet slices from the diffuser are pressed in screw presses to squeeze as much juice as possible out of them. This juice is used as part of the liquid in the diffuser and the pressed beet, by now a pulp, is sent to a drying plant where it is turned into pellets, which are a constituent of some animal feeds.¹⁵

The juice must now be cleaned up before it can be used for sugar production. This is done by a process known as carbonatation, where a lot of the non-sugars are collected and eliminated. Once this is done, the sugar liquor is ready for sugar production except that it is very dilute. The next step is evaporation to concentrate the liquor.¹⁵ Syrup obtained from evaporation is boiled until conditions are right for sugar crystals to grow, be separated, dried and packed.

Polarimetric Measurements for Quality Assessment

Since the process for sugar manufacture involves extraction, evaporation and crystallization steps, the yield and quality of the final product must be controlled and evaluated. There are a number of measurements that contribute to assessing optimized production and quality of sugar obtained from sugar cane or beets:

1. Pol (sucrose) percent in juice;
2. Pol (sucrose) percent in sugar cane or beets;
3. Brix (total soluble solids) percent in juice;

4. Brix percent in sugar cane or beets;
5. Fiber percent;
6. Commercial sugar (CS); and
7. Purity

Sucrose content is often referred to as % Pol, with Pol being derived from polarimetric measurements. Determination of % Pol in sugar cane and beet products is an important task. However, polarimetry is time consuming and in some cases, prone to underestimation. It is necessary to remove non-sucrose compounds, especially colored ones, in order to determine the sucrose content in different stages of the production.⁶

Sample clarification is achieved usually using lead salts, which are inconvenient because lead is a pollutant. For this reason, there have been several proposed methods to get around the use of lead, such as the use of aluminum-based clarifying agents, ultra filtration techniques and near infrared spectroscopy combined with multivariate statistical techniques.^{7, 16, 17, 18, 19, 20} Once the samples have been clarified, optical rotation measurements are made and % Pol in juice is obtained. Either a conversion table, like the one shown in Table 1, or a formula can be used to obtain the sucrose % in cane, juice and molasses. To use the table, the Brix, or total soluble solids, in juice must also be known. Brix is measured using a Brix spindle, density meter or refractometer. For example, a sample that has a Brix reading of 21.0 and a polarimeter reading of 75° equates to 17.98% sucrose in juice. The formula to calculate % Pol in juice is:

% Pol (sucrose) in juice =

$$\{-6.517 + (25.3 \times \text{PR}^*) - 0.0118 \times (\text{PR})^2 + (2.937 \times \text{Brix}) - 0.207 \times (\text{Brix})^2\} / 100$$

*PR = polarimeter reading

Table 1. Chart used to determine sucrose content from % Pol and Brix values.

Polarimeter reading	Brix								
		19.0	19.5	20.0	20.5	21.0	21.5	22.0	22.5
	71	17.16	17.13	17.09	17.05	17.02	16.99	16.95	16.92
	72	17.41	17.37	17.33	17.30	17.26	17.23	17.19	17.16
	73	17.65	17.61	17.58	17.54	17.50	17.47	17.43	17.40
	74	17.89	17.85	17.82	17.78	17.74	17.71	17.67	17.63
	75	18.13	18.09	18.06	18.02	17.98	17.95	17.91	17.87
	76	18.37	18.34	18.30	18.26	18.22	18.19	18.15	18.11
	77	18.61	18.58	18.54	18.50	18.46	18.66	18.39	18.35

Calculating % Pol in juice is the first step in calculating % Pol in cane. The next step is calculating fiber percentage. Over a period of 24 hours, samples are collected immediately after the cane has passed through the shredder. These samples are combined, and a 500 gram sample taken.¹⁵ This 500 gram sample is put through a cutter grinder, then placed into a fiber machine where it is washed to remove soluble solids and fine dirt, and finally dried using hot air and weighed. The final weight divided by the initial weight provides a fiber percentage. After fiber percentage is determined, % sucrose and Brix in cane are determined. Cane is squeezed through a series of rollers to extract the juice. The first pair of rollers squeezes a higher proportion of the Brix and Pol than subsequent rollers. Sampling of juice is routinely performed at the first set of rollers. Therefore the first step is to correct the Brix and Pol measurements in the first expressed juice to more accurately represent those of the total juice. This is done multiplying the Brix and Pol values in first expressed juice by 0.95.¹⁵ The second step is to account for the fiber percentage of the cane. This determination is important since higher levels of fiber make it more difficult to extract the juice in cane, and lower levels of fiber make it easier for the rollers to squeeze out a larger proportion of the total juice. Fiber per cent is

then deducted from a value of 100 (representing all components of cane) and divided by 100. Finally the corrected Brix and Pol in cane values are multiplied by the fraction of cane that is not fiber.

Commercial cane sugar (CCS) is calculated knowing both Brix and Pol in cane. CCS was originally known as POCS or pure obtainable cane sugar. CCS provides an estimate of the percentage of recoverable sucrose from cane. When calculating CCS it is assumed that 25% of the impurities in cane are removed in clarification and the remaining 75% is in molasses. For every 60 parts of impurities going to the molasses, 40 parts of sugar are also removed. As a result high impurity cane reduces the potential for raw sugar production, which has an increasing demand due to its lower exposure to clarifying agents.

Recent Methods for Sucrose Determination

Several new methods for the determination of sucrose are being introduced in the sugar industry. The polarimetric procedure requires removing non-sucrose compounds in order to minimize turbidity and color. Therefore, an important step is clarification. This is achieved by sedimentation of interferences using lead salts as a flocculating agent, the most widely used being lead subacetate, $\text{Pb}(\text{O}_2\text{CCH}_3)_2 \cdot \text{Pb}(\text{OH})_2$. The most recent methodologies are substitution of aluminum salts for lead salts, and use of near infrared spectroscopy to minimize sample preparation. In the conventional procedures, lead subacetate is added directly to the sample to be clarified. The proportion to be used is 2-3 g of the lead reagent for every 100 g of sucrose. The solution is stirred and let set until a white precipitate is formed, which is removed by filtration. The clear filtrate is then analyzed polarimetrically.⁶ Friedemann and coworkers studied the removal of a variety

of substances by using a reagent containing 10% HgSO_4 and 10% $\text{ZnSO}_4 \cdot 7\text{H}_2\text{O}$ in 1 *N* H_2SO_4 . With this reagent they were able to remove 70 to 99% of the color from molasses and juice. However the procedure is time consuming and requires the use mercury.²¹

According to Kishihara and others, an alternative for clarifying sugar cane juice is ultra filtration. The procedure requires asymmetric organic membranes. These types of membranes work at low pressures, and include cellulosic polymers, polypropylene, polysulfones, and polyamides. The choice of material will influence contaminant rejection characteristics, durability and fouling potential.¹⁶ For clarification of sugar samples, Kishihara and coworkers used a dynamic membrane formed on a porous ceramic tube. Despite a superior permeation flux, the residual color of the ultra filtrate was slightly inferior.¹⁶ Recently, Gyura and coworkers studied the substitution of aluminum sulfate for lead subacetate. Aluminum sulfate was added at different stages of the process and its effect on the quality of the molasses and juice was analyzed, determining the feasibility to substitute the lead subacetate.⁷

Sample preparation can be simplified even more by avoiding the use of clarifying agents. Recent methods involve spectrophotometric determinations and near infrared spectroscopy. NIR is appearing as a strong alternative for the analyses of colored solutions since the presence of color won't interfere in this region of the electromagnetic spectrum, and the data might be combined with multivariate statistical analysis to predict Pol values.^{18, 19, 20, 21}

Zagatto and coworkers determined sucrose spectrophotometrically in cane juice and molasses. The procedure involves filtration of the sample, and no clarification is required. The sample is introduced into a flow-injection analyzer designed with two

merging streams, producing two sample zones. One zone flows directly to the merging-stream confluence. The other zone is first heated at a coil in which sucrose is partially inverted with high reproducibility. At the confluence point, a buffered periodate stream is added to oxidize the sugar. The consumption of periodate is measured spectrophotometrically. The two processed zones proceed sequentially to a flow cell and two peaks are recorded. The sucrose content in the sample is proportional to the difference in peak heights.²²

Infrared spectroscopy is being used more frequently in the food industry. Based on reference polarimetric values, Maalouly and coworkers used outer product analysis (OPA) and 2D correlation spectroscopy (2DCOS) to determine regions of interest in sucrose spectra.²⁰ Outer product analysis can be used to facilitate the interpretation of near-infrared (NIR) and mid-infrared (MIR) signals. 2D correlation spectroscopy can be used to allow bands in the NIR spectrum to be resolved and assigned to characteristic absorbances in the MIR spectrum.²⁰ The principle of this method is to detect regions in both spectra (NIR and MIR) that change simultaneously as sugar content varies. Because NIR and MIR are used, clarification is not needed. Roggo and coworkers analyzed 2412 samples of sugar beet and built a predictive model based on near infrared reflectance spectroscopy, using spectral pre-treatment by a mathematical transformation of $\log(1/R)$. With this model, recorded spectra were corrected for particle size and color. NIR reflectance was concluded to be an alternative to polarimetry in the sugar beet industry.²⁰

Tewari and coworkers used FTIR in the mid-IR range to determine the Pol value in clear raw sugar cane juice. The method was combined with multivariate statistical analyses to predict the Pol value. With this technique, they were able to develop a

calibration model with a correlation $R^2 = 0.936$ using partial least squares regression.²⁴ IR spectroscopy has been used to determine sucrose and other sugars in other matrices. Miyamoto and Kitano used NIR transmittance spectroscopy as a non-destructive technique to determine sugars in mandarine juice.¹⁷ Rambla and coworkers combined partial least squares regression and NIR to determine total sugars (sucrose, glucose and fructose) using a model of binary and ternary sugar solutions with a 2.3% of maximum deviation.²² Other cases include the study of honey adulteration and invert cane using MIR spectroscopy.²⁵

Use of polarimetry also continues to be an active area of research. Kuchedjda and coworkers studied NIR polarimetry as a means to improve analytical techniques for sucrose determination.⁸ The method requires correction for color by previous calibration using international color units. Special interest in this technique has been shown in the South African sugar industry, where it is a goal to replace classical polarimetry with modern methods.²⁶ Schoonees and Alborough studied the feasibility of NIR polarimetry comparing it with polarimetry in different centers of the Cane Testing Service in Durban. Both studies concluded that sample preparation can be minimized to simple filtration, and color is a minimal interference.²⁶ The additional versatility of NIR polarimetry was established by Singleton and coworkers for simultaneous determination of dextran and sucrose. Dextran presence indicates loss of sucrose. Its appearance is associated with microorganisms that consume sugar and produce dextran as a metabolic residue.²⁷

Optical Activity Measurements in the Pharmaceutical Industry

Another field of application for optical activity measurements is enantiomeric discrimination, which has special relevance in the pharmaceutical industry. The

separation and quantification of enantiomers is difficult to achieve. However, they can be distinguished optically by means of polarized light.⁵ The majority of pharmaceutically active compounds are usually small chiral molecules. The chirality of these agents is normally evaluated using polarimetry, where the sign and magnitude of the specific rotation are used to confirm the enantiomeric identity and/or purity of the analyte.²⁸ The velocity of light passing through a medium is determined by the index of refraction of that medium. For an achiral medium, the refractive index will not exhibit a dependence on the sense of the polarization state of the light. When the medium is chiral, however, the refractive index associated with left-circularly polarized light will not equal the refractive index associated with right-circularly polarized light, and the velocities of both polarized beams will differ. Since linearly polarized light is the resultant of two circularly polarized components in-phase, then the differing velocities of the components will produce a phase difference as they pass through the chiral medium. On leaving the chiral medium, the components are recombined, and linearly polarized light is obtained whose plane is rotated (relative to the original plane) by an angle equal to half the phase angle difference of the circular components.²⁸ The magnitude of the angle of rotation depends on the wavelength of the light used, which gives rise to ORD curves that are characteristic of molecules with pharmaceutical significance, and for which regulatory agencies require measurements of optical activity as one proof of chiral identity.

CHAPTER THREE

Theoretical Considerations

When ordinary unpolarized light passes through a polarizer, like a Glan-Taylor prism, it becomes linearly polarized. When light is linearly polarized, the plane of the electric vector of the light wave is restricted to a particular plane that depends on the orientation of the polarizer. If a second polarizing prism is placed after the first, the intensity of light passing out of the assembly will vary as the second prism is rotated about its axis. According to Malus' law, the intensity of light passing through the pair of polarizers will vary as $\cos^2 \beta$, where β is the angle between the two polarizers. When the planes of the two polarizers are coincident, the light intensity that passes through the combination will be a maximum. When the planes of the two polarizers are at 90° , the light intensity will be a minimum, as shown Figure 12.⁵

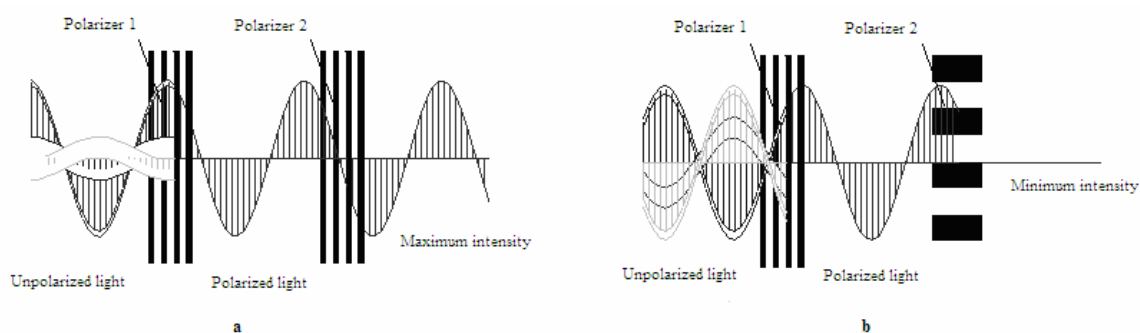


Figure 12. Representation of the change in intensity of a beam crossing a set-up of a. two parallel polarizers and b. two perpendicular polarizers.

Suppose that a polarimeter is arranged so that the two polarizers are at 90° to one another. In this condition, no light should pass through the second polarizer (Figure 12.b). If an optically active sample is placed between the two polarizers, it will rotate the plane of polarized light so that some light passes through the second polarizer (the analyzer). If the analyzer is rotated so that the light is once again extinguished, the angle by which the polarizer was rotated is the optical activity of that sample.²⁸ Now consider two ideal polarizers arranged so that their planes of polarization are at a 45° angle, as shown in Figure 13.

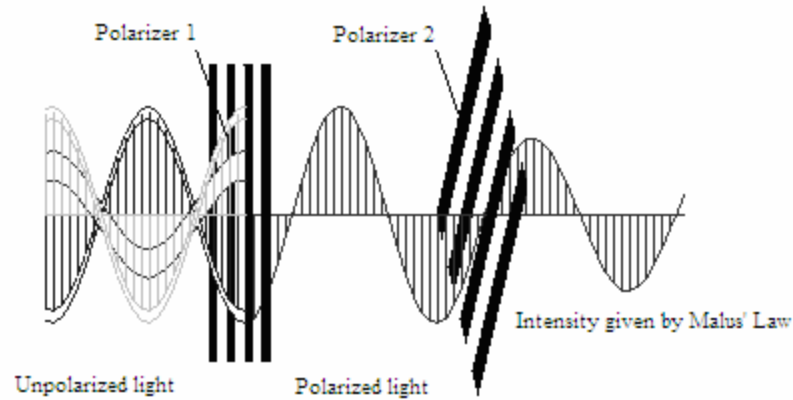


Figure 13. Set-up of two polarizers at a fixed angle of 45 degrees.

According to Malus' law, in this situation the intensity of light passing through the combination should be

$$I^0 = k \cos^2 45^\circ \quad (3.1)$$

where k is a constant of proportionality. If an optically active sample is placed between the polarizers, it will rotate the plane of polarization of the light incident on the second polarizer. Thus, when a transparent optically active sample is placed between the polarizers,

$$I = k \cos^2 (45^\circ \pm \theta) \quad (3.2)$$

where θ is the optical rotation due to the presence of the chiral sample. The \pm sign refers to the direction of the rotation (i.e., did the sample rotate the light so that the total angle (α) increased or decreased). According to Equations 3.1 and 3.2, the absorbance produced by the presence of the transparent optically active sample will be given by

$$A = -\log (I/I^0) = -\log \{(\cos^2 \alpha)/0.50\} = -\log (2\cos^2 \alpha) \quad (3.3)$$

where α is $45^\circ \pm \theta$.

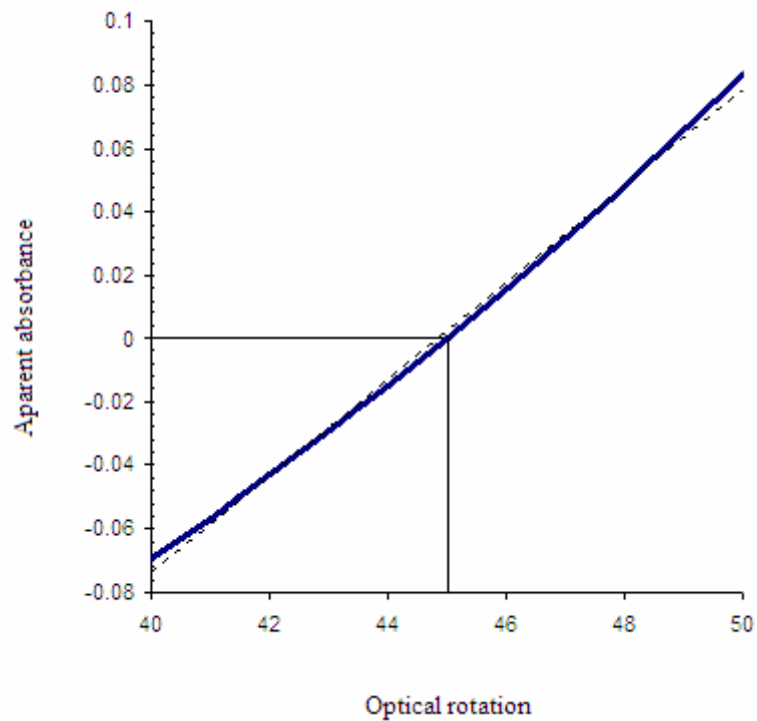


Figure 14. Ideal plot of change in absorbance as function of the optical activity.

Figure 14 shows a plot of apparent absorbance A versus α as θ varies between 0 and $\pm 5^\circ$ (α goes from 40° to 50°). From the plot, it can be seen that the absorbance produced by the optical rotation of the chiral sample varies nearly linearly with the optical rotation θ itself. The proposed spectropolarimetric configuration makes use of this property. Equation 3 will not apply if the chiral sample contains colored material

that also produces an absorbance. This problem can be eliminated by background correction procedures described in the experimental section.

An ordinary polarimeter generally makes measurements at a single fixed wavelength. Historically, polarimetric measurements were made at 589 nm. Today, modern instruments often have a number of wavelengths available that can be used, and with the availability of spectropolarimeters, the variation of optical rotation can be studied over a range of wavelengths. Use of multi-wavelength data from spectropolarimetric measurements can provide additional information about a sample from optical rotatory dispersion curves characteristic for each chiral analyte. If a sample is colored so that the intensity of light passing through it is reduced appreciably, ordinary polarimetry becomes problematic because it is difficult to discern the null condition. In the case of using polarimetry to determine sugars, the presence of color in sugar samples like cane sugar and beet sugar causes problems.

Another type of measurement done routinely in the sugar industry is to follow the inversion of sucrose, which is also affected by the presence of color. Inverted sugar is of special interest due to its increased sweetness over ordinary sucrose. Because of the differences in optical activities of the inversion products with respect to sucrose, the rate of inversion can also be followed polarimetrically. A general polarimetric procedure is explained by Daniels.³⁰ For the particular case of the set-up presented in this work, sucrose inversion is followed spectrophotometrically measuring the apparent absorbance at different times, in an analogous way to the polarimetric method. Sucrose is a disaccharide that undergoes hydrolysis in an acidic medium. The products of the

hydrolysis are the monosaccharides glucose and fructose. This process is known as inversion. The rate law for the inversion of sucrose is:³⁰

$$d[\text{sucrose}]/dt = k [\text{sucrose}]^m [\text{H}_2\text{O}]^n [\text{H}^+]^p \quad (3.4)$$

From Equation 3.4 it can be seen that the rate of inversion depends on the concentrations of sucrose, water and acid. In acidic aqueous media, the concentrations of water and acid can be made to be essentially constant. So Equation 3.4 can be re-written to specify the dependence on the concentration of sucrose only:³⁰

$$-d[\text{sucrose}]/dt = k_{\text{eff}} [\text{sucrose}]^m \quad (3.5)$$

where

$$k_{\text{eff}} = k [\text{H}_2\text{O}]^n [\text{H}^+]^p \quad (3.6)$$

Under the specified conditions (water is in excess and the acid is in a concentration equal to 4 M), it can be shown that the reaction is pseudo first order in sucrose ($m=1$), which is verified by fitting the experimental data to a first-order integrated rate law. In the equations that follow, $[\text{sucrose}] = c$. It is assumed that the reaction goes to completion so that practically no sucrose remains at "infinite" time. The integrated form of the first-order-reaction differential equation is then:³⁰

$$c = c_0 e^{-k_{\text{eff}} t} \quad (3.7)$$

where c_0 is the concentration of sucrose at the beginning of the reaction. Taking logarithms,

$$\ln(c/c_0) = -k_{\text{eff}} t \quad (3.8)$$

Thus the slope of a plot of $\ln c/c_0$ versus t is $-k_{\text{eff}}$. However, in this experiment the concentration of sucrose is not directly measured. Instead apparent absorbance is measured. Absorbance is directly proportional to concentration. Using the crossed

polarizers set-up described in a previous section, the inversion of sucrose is followed in a similar way to that in which this process is followed polarimetrically. The crossed polarizer set-up allows the measurement of absorbance as an equivalent of the angle of rotation, even in colored samples of sucrose. A more detailed explanation can be found in the Appendix.

For other optically active samples, background correction might be useful to identify one enantiomer over the other based on the optical rotatory dispersion spectrum of a mixture of both. Even more, if the method combines the proposed background correction with multivariate statistical regression over an appropriate range of wavelengths, it could be possible to predict simultaneously total concentration and enantiomeric composition, because the spectrum of a mixture is the result of the combined apparent absorbances of both enantiomers. This situation holds regardless of the total concentration. This outcome is different from other multivariate regression models, where the total concentration was kept constant and the prediction was made based on different enantiomeric compositions.

CHAPTER FOUR

Experimental Section

Apparatus

The instrument is based on an ordinary UV-visible spectrophotometer (Agilent 8453 UV-visible spectroscopy system),²⁹ that can accommodate long pathlength cells. The device uses a solid-state array detector to detect a spectral range from 200-1100 nm, thus providing multiwavelength information. Optical rotation is observed in terms of the apparent absorbance. Since absorbance is an additive property, corrections for colored samples were accomplished without need for chemical pretreatment.

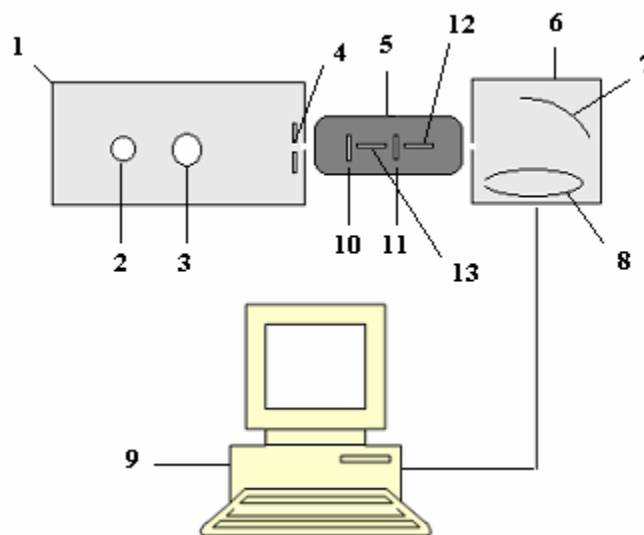


Figure 15. Schematic representation of the spectropolarimetric set-up.

Figure 15 shows a schematic diagram of the instrument. Housing **1** is a compartment for the light sources of the spectrometer. Lamp **2** is a quartz-halogen lamp that produces light in the visible and near-IR regions of the spectrum, thereby providing spectral coverage from 400-1100 nm. Lamp **3** is a low-pressure deuterium arc that produces light in the ultraviolet region of the spectrum (200 – 400 nm). The lamps are arranged so that their radiation forms a single beam that passes into the sample compartment **5**. A shutter **4**, operationally connected to the computer **9** allows light to pass from the lamp housing **1** for a predetermined exposure period when the spectrometer is activated. The sample compartment **5** contains a specially-designed sample holder **12** for a 20 mm sample cell **13**. The sample holder is made so that the sample cell can be uniformly and reproducibly placed in both locations. Also on the sample holder are two Glan-Taylor prism polarizers **10** and **11**. These polarizers have an extinction coefficient of 5×10^{-5} , work in a range of wavelengths between 215 nm and 2300 nm, and are fixed in the sample holder with their planes of polarization at a 45° angle to one another. Following the sample holder is a polychromator **6** equipped with a concave holographic grating **7** and a solid-state array detector **8**. The output from the solid-state array detector is operationally connected to the computer **9** to compute the absorbance spectrum of the assembly.

Polarimetric measurements were done with an Autopol® III, Automatic Polarimeter, Rudolph Research with a 1 dm cell, which offers six different wavelengths to acquire angles of rotation.

Reagents

Sucrose Determinations

Sucrose solutions were prepared without previous purification or drying of sucrose. Reagent grade sucrose was from Mallinckrodt Chemicals, basic lead (II) acetate, ACS from Alfa Aesar, and samples of raw sugar, organic sugar, light brown sugar and dark brown sugar were of commercially available brands. Reagent grade hydrochloric acid, EMD™ lot # 45236 was used as the catalyst in sucrose inversion.

Enantiomeric Discrimination

Three pairs of enantiomers from Aldrich Chemical Co. Inc. with enantiomeric purity over 96% were used. The studies were based on (*R*)-(+)-limonene, (*S*)-(-)-limonene, L-arabinose, D-arabinose, (*R,R*)-(+)-*N,N'*-bis(α -methylbenzyl)sulfamide and (*S,S*)-(-)-*N,N'*-bis(α -methylbenzyl)sulfamide. Reagent grade methanol was from Alfa Aesar.

Experimental Procedure

For sucrose determinations all solutions were prepared by direct gravimetry and diluted in deionized water. Polarimetric measurements were made directly on the colorless solutions. Colored samples were clarified according to the recommended procedure.⁶

Racemic mixtures of limonene and arabinose were prepared, respectively. Known amounts of the respective dextrorotatory enantiomer were added to a fixed volume of each racemic mixture, therefore changing enantiomeric composition and concentration simultaneously. Reagent grade methanol was used to dissolve limonene and *N,N'*-bis(α -methylbenzyl)sulfamides. Arabinose was dissolved in deionized water.

Spectropolarimetric measurements were done with previous background correction in two ways: 1) using water as a blank and 2) using the solutions as their own blank. Figure 16 shows an expanded view of the sample holder **5** from Figure 15.

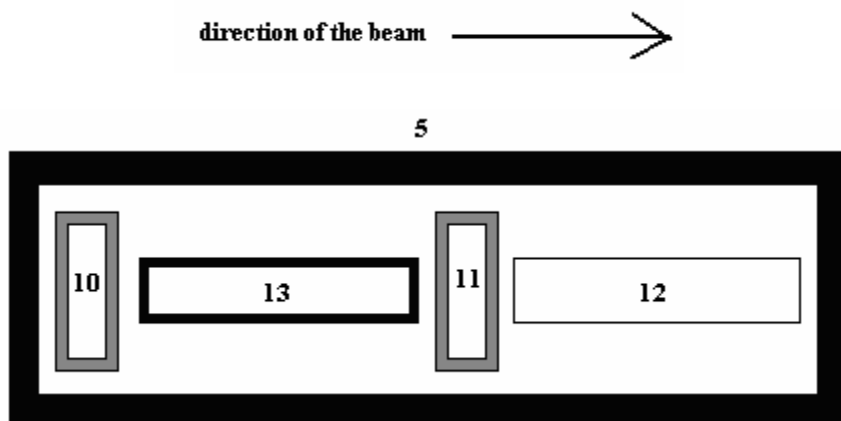


Figure 16. Expanded view of the sample holder arranged with a crossed polarizers set-up.

When water was used as a blank, the cell was filled with deionized water and placed in position **13** in the cell holder. With the cell in this position the blank spectrum was recorded. Samples' spectra were recorded replacing deionized water with the samples in the same position.

Alternatively, each solution was used as its own blank. The sample was placed in position **12** in the sample holder, after the pair of polarizers **10** and **11** as shown in Figure 16. This configuration was used to record the blank for each solution. After this blank was recorded, the cell was placed in position **13** of the sample holder, between the two polarizers, and a second absorbance spectrum was acquired and saved.

Sucrose concentration and enantiomeric excess were determined by multivariate regression models based on partial least squares using The Unscrambler®. To make the models, a series of colorless calibration samples of known concentration were prepared

and their optical rotatory dispersion spectra were recorded using both background correction procedures for sucrose: 1) using a water blank and 2) using each solution as its own blank. Enantiomeric excess determinations were performed using each solution as its own blank only. Unknown samples' spectra were recorded and inputted in the respective calibration models and predicted for sucrose concentration or enantiomeric composition, respectively. Sucrose inversion measurements were made using each solution as its own blank on colorless sucrose solutions at 589 nm, and on dark brown sugar at 850 nm. Results were fitted using MS-Excel solver expanding the scale 1000 times.

Spectropolarimetric results were compared with polarimetric measurements. Polarimetric determinations of sucrose were made directly at 589 nm for colorless samples, and with previous clarification using lead sub acetate for colored samples at the same wavelength. Inversion of sucrose was also followed polarimetrically at 589 nm also, except for dark brown sugar, which was not studied using this method. Fragments of the ORD curves were generated at the six possible wavelengths of the Autopol III polarimeter in the enantiomeric discrimination studies, and compared with the spectropolarimetric measurements.

CHAPTER FIVE

Results and Discussion

Sucrose Determination

An ORD curve shows the variation of optical rotation with wavelength. This information is typically recorded using a spectropolarimeter, which consists of a polarimeter that operates at a range of wavelengths. Modern conventional polarimeters also offer the possibility to measure the angle of rotation at several non-continuous wavelengths, usually five or six more than a single wavelength instrument. This feature allows them to operate in a limited spectropolarimetric mode. Figure 17 is a fragment of the ORD curve of sucrose between 350 to 650 nm. This fragment shows that angles of rotation decrease as wavelengths increase, which is the expected behavior.¹¹ It was generated from angle of rotation measurements at each of the six wavelengths of operation of an Autopol III polarimeter.

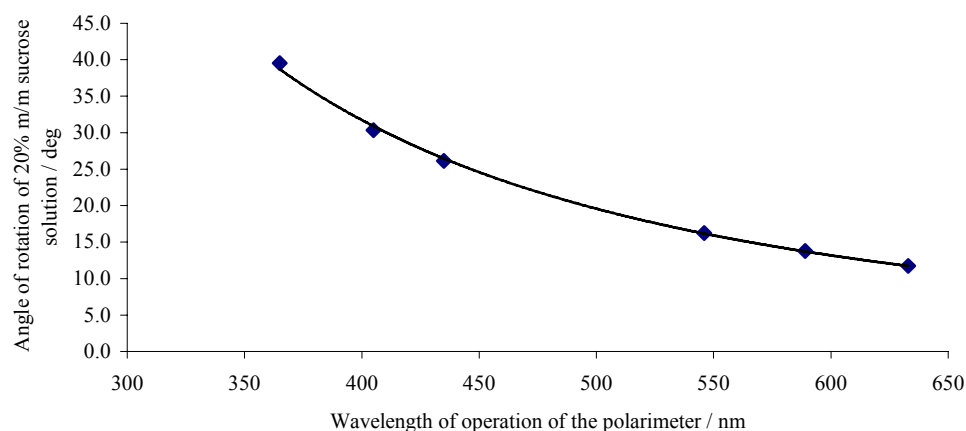


Figure 17. Fragment of the optical rotatory dispersion (ORD) curve of sucrose generated from the wavelengths of operation of a Rudolph Autopol III Polarimeter.

In an arrangement of crossed polarizers at a fixed angle of 45° , according to Malus' Law apparent absorbance should be equivalent to angle of rotation at a given wavelength. Figure 18 is an analogous ORD-type curve generated using the crossed polarizer spectrophotometric set-up. This plot was constructed taking the measured apparent absorbances at the same wavelengths of operation of the polarimeter. Comparing Figures 17 and 18 it is observe that angle of rotation and apparent absorbance follow the same behavior with respect to wavelength.

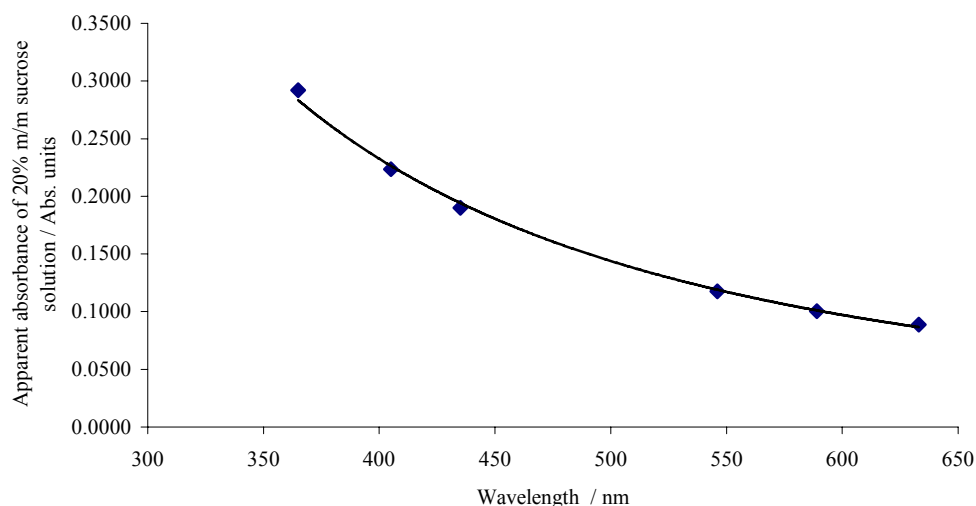


Figure 18. Fragment of an ORD spectrum –absorbance vs. wavelength- of sucrose, generated from the wavelengths of operation of a Rudolph Autopol III Polarimeter.

An important outcome of this spectrophotometric set-up is the possibility of its use as a spectropolarimeter, capable of generating pseudo-absorption spectra equivalent to optical rotatory dispersion curves. Figure 19 shows the correspondence between apparent absorbances shown in Figure 18 and the measured angles of rotation in Figure 17, at each of the polarimetric wavelengths. The polarimetric measurements are considered as the reference.

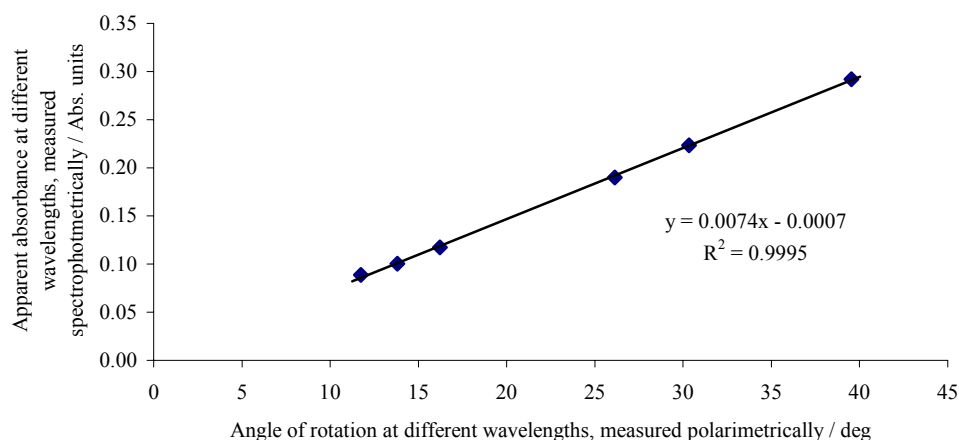


Figure 19. Absorbance vs. angle of rotation at the polarimetric wavelengths.

The result shown in Figure 19 not only confirms that the pseudo absorption spectra recorded using a crossed polarizers set-up at a fixed angle is equivalent to an ORD curve, but also that absorbance is nearly linearly related to optical rotation as describe by Malus' Law:

$$A = -\log (2\cos^2 \alpha) \quad (5.1)$$

where A is apparent absorbance and α is the optical rotation for a fixed polarizer angle of 45° . According to this relationship absorbance decreases as the angle of rotation decreases, which is obvious from the ORD curve. The linear relation shown in Figure 18 is modeled empirically by:

$$A = 0.0074 \alpha + 0.0007 \quad (5.2)$$

where A and α have the same meaning as in Malus' Law, and show a linear correlation of 0.9995 between the two instruments. The equivalence between polarimetric angles of rotation and apparent absorbances measured with the new spectropolarimeter is supported in Figures 20 and 21 at different concentrations.

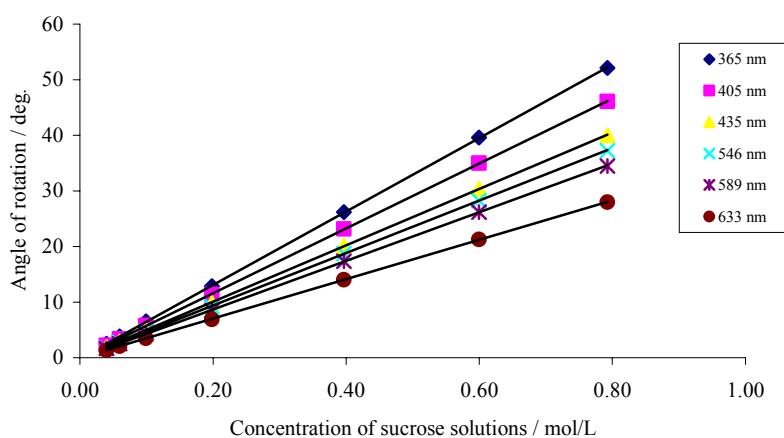


Figure 20. Angle of rotation vs. concentration as recorded polarimetrically.

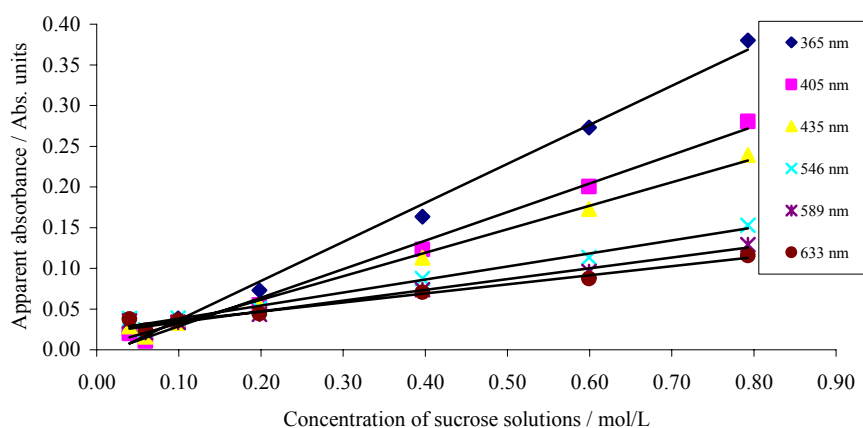


Figure 21. Apparent absorbance vs. concentration. Plot generated using a crossed polarizers spectrophotometric set-up, at the polarimetric wavelengths.

For polarimetric measurements, the relationship between angle of rotation and concentration follows the equation:⁵

$$\alpha = [\alpha]_{\lambda}^T * c * \ell \quad (5.3)$$

In spectrophotometric measurements, a similar relationship holds based on the Beer-Lambert Law:⁵

$$A = \epsilon * c * \ell \quad (5.4)$$

Figures 20 and 21 show that the equivalence between angle of rotation and apparent absorbance using the proposed set-up, hold for a range of concentrations. Figure 21 shows the same trend as does Figure 20 based on polarimetric measurements, and the ORD nature of the plots is revealed by the fact that even at different concentrations, as the wavelength increases, the angle of rotation and the apparent absorbance decrease.

Figures 17 and 18 showed previously, are fragments of the ORD of sucrose at specific wavelengths. In a continuous spectral range, ORD curves are useful chiroptical pieces of information for optically active compounds that have no chromophores. Figure 22 shows the complete ORD spectrum of sucrose, from which Figure 18 was taken.

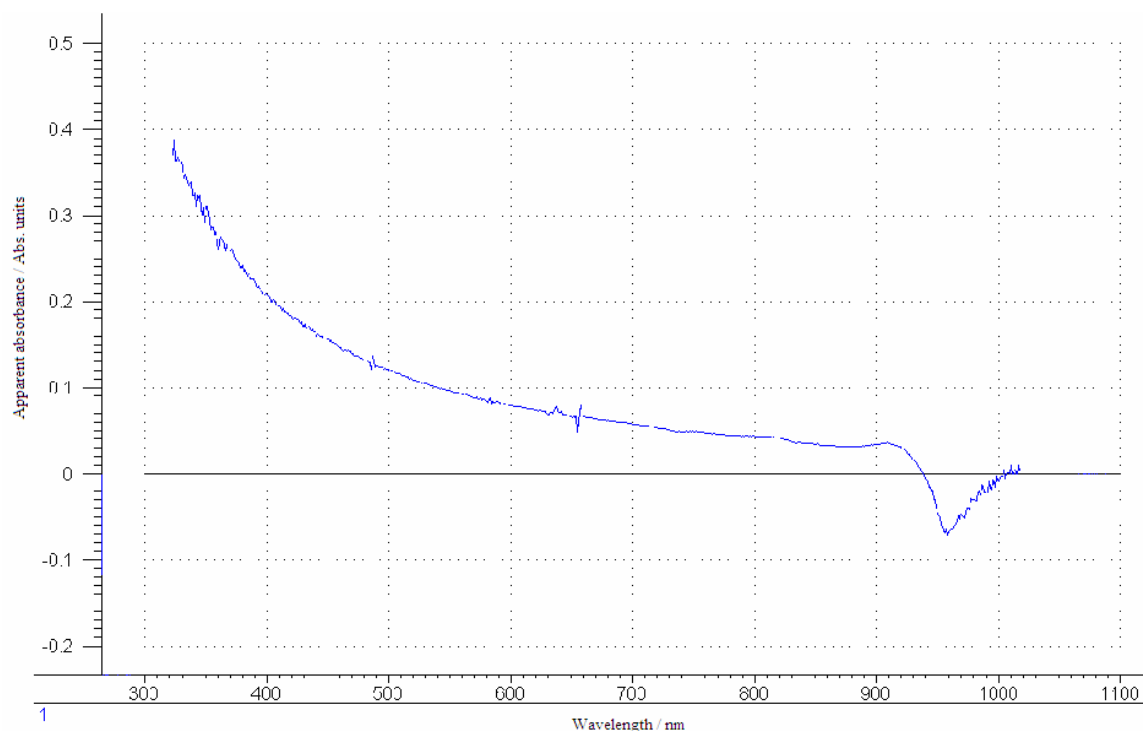


Figure 22. Optical rotatory dispersion spectrum for 20% by mass in sucrose recorded using the new spectropolarimetric arrangement.

In the range from 350 to 650 nm Figure 22 shows a typical ORD behavior, which holds up to approximately 900 nm. At 960 nm a band due to water is observed.

According to Rambla, the negative absorbance in Figure 22 at 960 nm is probably due to a decrease in the concentration of water in the solution with respect to the blank.²² Golic and coworkers observed a similar behavior in the short-wavelength NIR spectrum of sucrose, and reported a band at 970 nm due to –OH stretching. In both cases the band was not observed by means of an interaction with polarized light,³¹ which is not the case of Figure 22 that was recorded using crossed polarizers at a 45° angle.³² So the presence of a band at 960 nm might be related to the use of water as a blank.^{22, 31}

The previous result suggests that background correction using a water blank does not isolate the absorption due only to optical rotation and other factors are causing the apparent absorbance to decrease. Instead of using a water blank, improved background correction was achieved using the solution as its own blank simply changing the position of the cell in the cell holder. Figure 23 shows the spectrum of sucrose using water as a blank, at a different sucrose concentration from Figure 22. It shows clearly the optical rotatory dispersion of sucrose between 300 nm and 900 nm, and the apparent absorbance shows the same negative value as in Figure 22 approximately at 960 nm. When background correction is done by moving the cell, the change in absorbance due to rotation is isolated from other absorbing factors, such as solvent effects and hydrogen bonding between sucrose and water. Figure 24 shows the ORD for the same solution used to generate Figure 24, but with background correction using the sample as its own blank. In this case no –OH band is observed at 960 nm, and the spectrum resembles a pure ORD curve.^{11, 33}

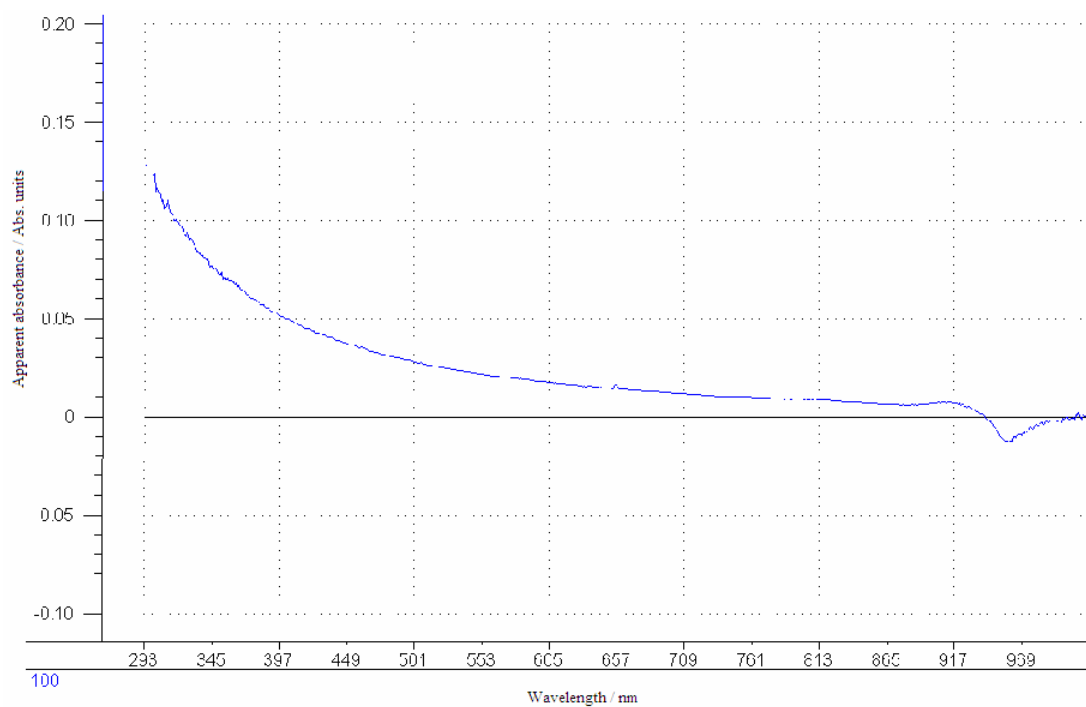


Figure 23. ORD-type curve for 5% w/w sucrose obtained using a novel polarized spectrophotometric set-up with a water blank.

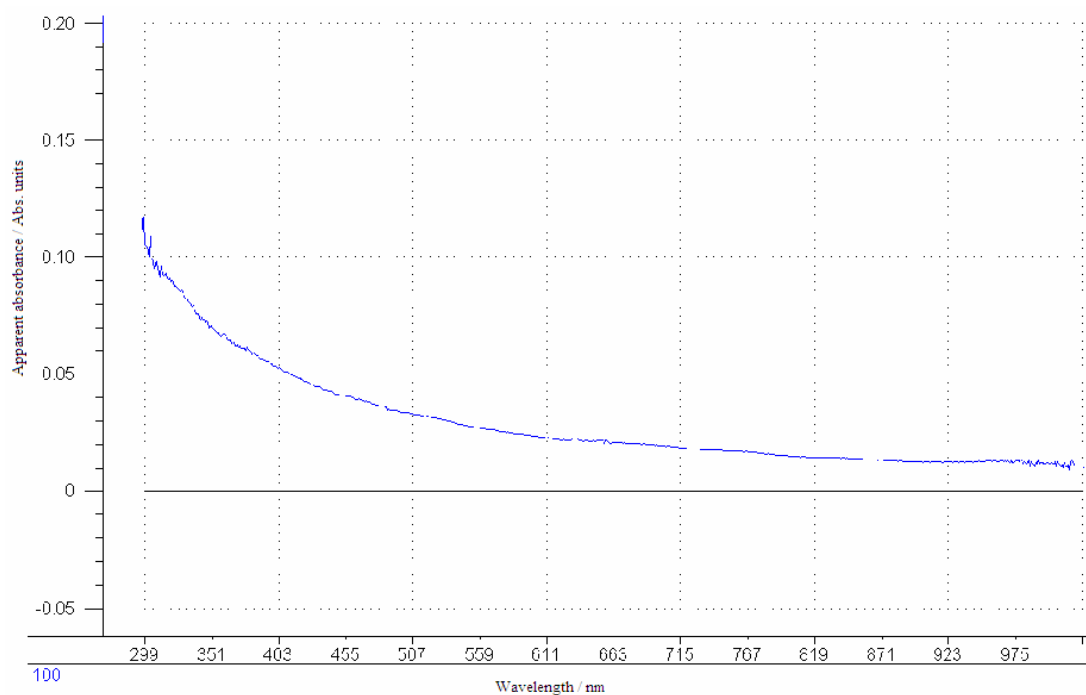


Figure 24. ORD curve for 5% w/w sucrose obtained using a novel polarized spectrophotometric set-up with the same solution as a blank.

Since absorbances are additive, an algebraic rationale is useful to understand the proposed background correction:

$$A = A_{(polarizers)} + A_{(water)} + A_{(sucrose / water)} + A_{(optical\ rotation)}$$

where A is the apparent absorbance of the set-up due to each factor specified. When the solution itself is used as a blank, the absorbance due to the polarizers, solvent and solute-solvent interactions (such as hydrogen bonding), are corrected leaving only:

$$A = A_{(optical\ rotation)}$$

The use of the solution as a blank shows a higher reproducibility than when water is used as blank. At 589 nm, the classical wavelength of polarimetric determinations, the standard deviation for absorbance is 0.00038 (n=10) in the first case, and 0.0027 (n=10) when water is used as blank. The capability of this novel arrangement for background correction, the absence of moving parts compared to a conventional polarimeter, and its mode of operation in a wide spectral range makes the new instrument versatile for sucrose determinations, especially for colored samples.^{13, 34, 35}

For the determination of colored samples, the polarimetric method requires previous clarification using lead subacetate. If background correction is done, absorbance due to rotation might not only be isolated from solvent related absorptions, but also from those due to the presence of achiral colored substances. Figure 25 shows a calibration curve used in the polarimetric determinations of sucrose. The linearity of the polarimetric method makes it suitable to obtain reference values for sucrose concentrations in different samples.

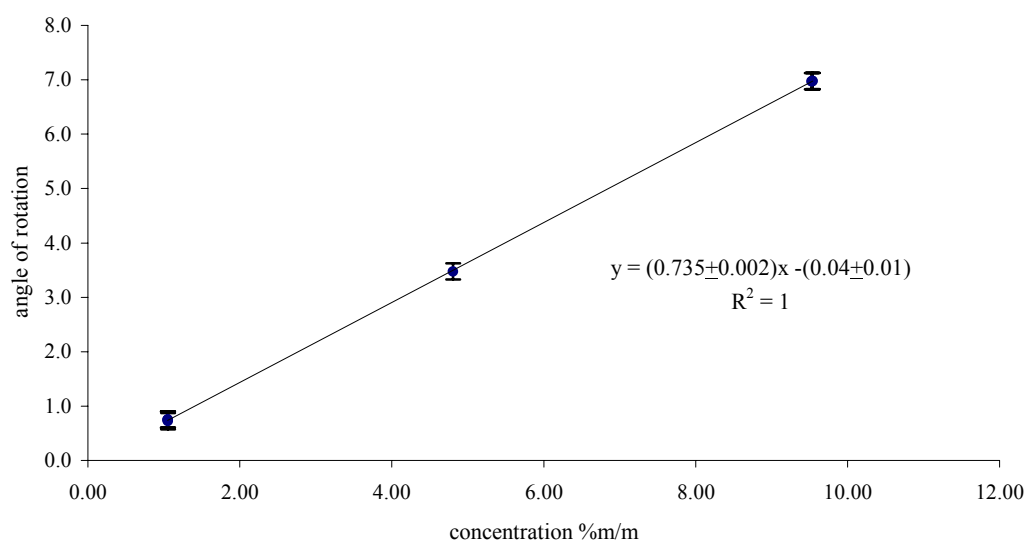


Figure 25. Calibration curve used for the determination of sucrose by polarimetry.

Table 2 shows sucrose concentrations expressed as % by mass determined by different methods.³⁶ The first column shows the results of polarimetric determinations used as a reference method at three levels of concentration for nine independent samples of pure sucrose. The other columns show the results obtained from two models based on partial-least-squares regression for a model based on a calibration set of 100 samples. The first model was made with water as a blank and the second one with background correction using samples as their own blank. Both models are shown in Figures 25 and 26, respectively. As can be seen in Table 2, the predicted values using background correction are in better agreement with the polarimetric results.

Table 2. Sucrose concentrations expressed as % by mass of pure sucrose using three different methods.

Sample	Reference % w/w	Polarimetric % w/w	% Error	Spectropolarimetric		Spectropolarimetric	
				% w/w predicted		% w/w predicted	
				without background	% Error	with background	% Error
				correction between 750 nm and 925 nm		correction between 750 nm and 925 nm	
1	1.92	1.98	3.13	2.92	52.1	1.82	-5.21
2	1.93	1.92	-0.52	2.70	39.9	1.80	-6.74
3	1.92	1.91	-0.52	2.72	41.7	1.62	-15.63
4	3.8	3.69	-2.89	4.79	26.1	3.62	-4.74
5	3.81	3.74	-1.84	5.71	49.9	3.71	-2.62
6	3.82	3.75	-1.83	5.54	45.0	3.81	-0.26
7	5.73	5.66	-1.22	6.96	21.5	5.83	1.75
8	5.73	5.67	-1.05	7.98	39.3	5.52	-3.66
9	5.73	5.65	-1.40	7.86	37.2	5.59	-2.44

Figure 26 is an output for partial-least-squares regression using the statistical software Unscrambler®. Linear regression was performed over a range of wavelengths between 750 nm and 925 nm. Instead of performing a regression based on one response variable (Y) and one predictor variable (X) as in Figure 25, this wavelength range includes a set of 175 absorbances for each sample (one absorbance for each wavelength from 750 nm to 925 nm). The multivariate nature of PLS enhances the reliability of regression models.^{37, 38, 39} Y variables are the concentrations of sucrose expressed as % by mass, and the X variables are the apparent absorbances. An Unscrambler® output such as the one shown in Figure 26, in general shows a plot of the predicted concentrations against the measured values (Figure 26.d). Measured values are those used as reference values from the direct preparation of the samples. Figure 26.c is a plot that gives an indication of how much of the variation in the data is described by the partial-least-squares (PLS) components. Figure 26.b shows the regression coefficients plot.

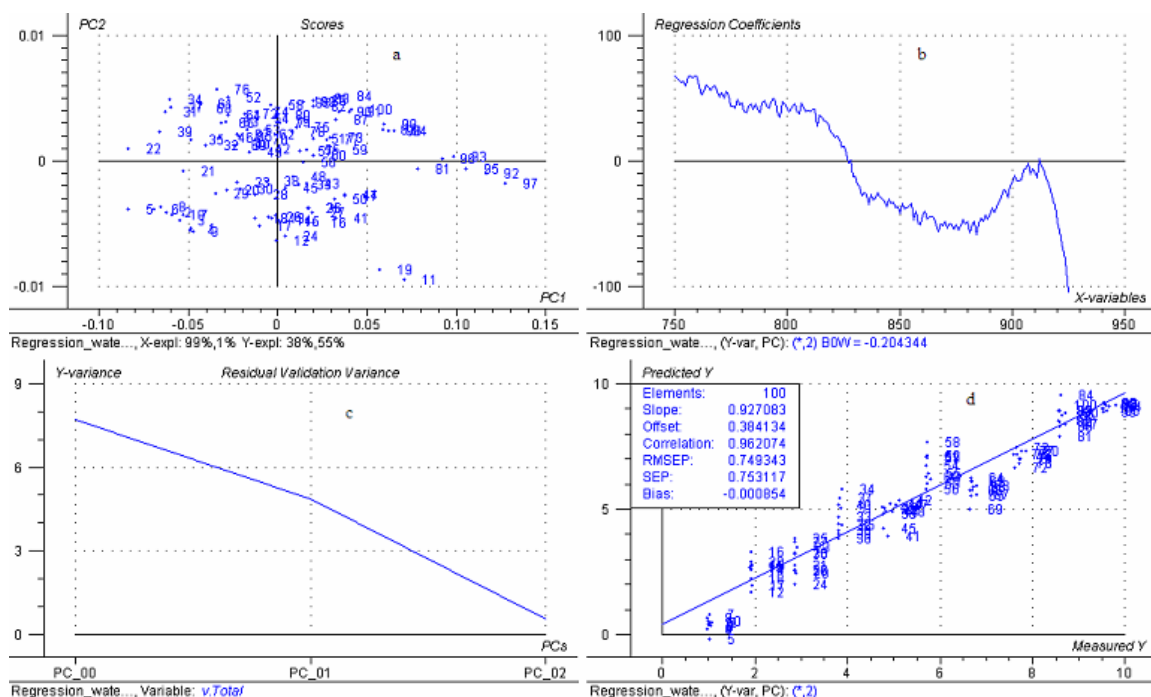


Figure 26. Multivariate regression model based on partial least squares, for a calibration set between 750 nm and 925 nm using water blank.

Table 2 above showed the results obtained for sucrose concentrations using the model without background correction in Figure 26. The plot of predicted concentration vs. measured concentration (Figure 26.d), shows a linear trend. The inset shows a good multivariate linear correlation of 0.9621 and a low offset. This plot lets us check the quality of the regression by showing the points close to a straight line. However, the PLS components (Figure 26.c) show an irregular behavior since the second principal component explains more of the variation for concentrations than the first principal component.³⁸ PLS components are a set of orthogonal variance-scaled vectors that can be used as a new basis set on which to represent the data.⁴⁰ Figure 26.a shows that the first principal component explains 38% of the variation in concentration (Y), and the second one explains 55%. This is an irregular result because in a linear regression based

on PLS1, the variance is expected to decrease as the number of principal components increase, as is the case with absorbances (X), where the first principal component explains 99% of the variation.

The regression coefficients plot (Figure 26.b) summarizes the relationship of all predictor variables with a given response variable. The main application of the regression coefficients is to build the regression equation and express the link between the variation in the absorbances and the variation in concentrations. A smooth plot suggests a stronger relationship between both kinds of variables. Some interactions that might originate in the use of water blank for background correction might be revealed in this plot. If this is the case, regression coefficients for this model are not accounting only for the interaction between sucrose and polarized light, but also for the background absorption from water. This is in agreement with the ORD spectra shown in Figures 23 and 24. Figure 23 showed an absorption band at 960 nm that is eliminated with background correction, being absent in Figure 24. The scores plot (Figure 26.a) does not show any specific grouping. Scores plots give information about patterns in the samples. The scores plot for the first two principal components is especially useful, since both summarize more variation in the data than any other pair of components. The closer the samples are in the scores plot, the more similar they are with respect to the two components concerned. Conversely, samples far away from the rest can be considered different from the others or even outliers.^{38, 39} Based on this criterion, Figure 26 suggests that samples 11 and 19 might be considered as outliers, but there is no additional evidence to support this.

When a new model is build using each sample as its own blank for background correction, the regression results improve. Figure 27 shows a new model using the proposed procedure of isolating the absorbance due to optical activity. In contrast to the model made with water as a blank, Figure 27 shows better graphical and numerical linearity (Figure 27.d). In Figure 26 a correlation of 0.9621 is obtained for multivariate calibration, where for Figure 27.d a value of 0.9866 is obtained. Also the PLS components (Figure 27.c) are “well behaved”. The first principal component explains 100% of the variation in absorbance, against 99% for the first model. And in the case of the variation in concentration, the first principal component explains 66% of the variability and the second one 31%. This is a more congruent than that in the first model.

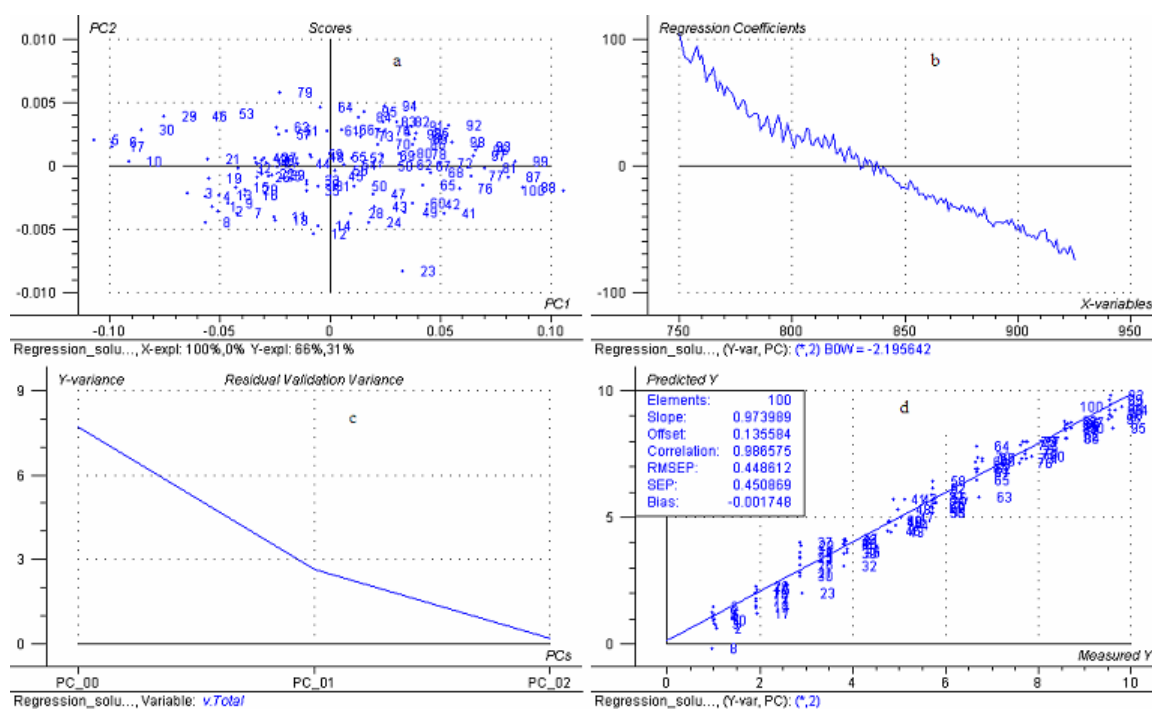


Figure 27. Multivariate regression model based on partial least squares, for a calibration set between 750 nm and 925 nm using background correction.

The regression coefficients plot (Figure 27.b) is more homogeneous than that in Figure 26.b. As expected from using the solutions as their own blank, the regression coefficients in this model might be accounting for a regression equation based only in the interaction between sucrose and polarized light. Also, the scores plot (Figure 27.a) shows more independency between samples for the first two principal components.

Since the model built using background correction gave better results than that obtained without such procedure, it can be inferred that this procedure might be useful for sucrose determinations in real samples that require clarification. Background correction performed as explained in the experimental section can be used to avoid the interferences due to colored achiral substances in sugar and other products. Other tested models were based on a calibration set of a lower number of samples, different wavelengths, and on light brown sugar. These are shown in the Appendix. Table 3 shows the results obtained in the analyses of colored samples. In Table 3 the reference values were obtained by conventional polarimetry with prior clarification.

Table 3. Sucrose concentrations expressed as % w/w in colored samples using background correction between 750 nm and 925 nm.

Sample	Reference % w/w	Polarimetric % w/w	% Error	Spectropolarimetric % w/w	% Error
Raw sugar	1.72	1.69	-1.74	1.67	-2.91
Light brown sugar	1.70	1.66	-2.35	1.67	-1.76
Dark brown sugar	1.78	1.67	-6.18	2.23	25.3
Coffee	1.69	1.69	0.00	2.35	39.1

The best predictions are those for raw sugar and light-brown sugar. Both types of sugar have the lowest color in this set of four samples. Figure 28 shows the relative colors of the samples with respect to pure sucrose. According to sugar manufacturers, light brown sugar and dark brown sugar have around 10 to 15% of invert sugar, which is not present in raw sugar. However, it is not specified if there are any other chiral absorbing compounds that might increase the obtained result.¹⁶



Figure 28. Colored sugar samples. From left to right: pure sucrose, raw sugar, light brown sugar, dark brown sugar and coffee.

In the case of the sample containing coffee, it was prepared by adding a known amount of coffee to a 1.69% w/w solution of pure sucrose. Before adding the coffee, it was measured polarimetrically. After the addition of coffee it was measured spectropolarimetrically. The increased result with respect to polarimetry might be related to the fact that the coffee used was roasted coffee. This kind of coffee is roasted mixed with sucrose, which will be present in an additional amount. This can be therefore a

potential procedure to determine sucrose in roasted coffee since the difference between a known amount of sucrose and the predicted result can give the amount of sucrose present in roasted coffee. Samples from Table 3 were predicted using a model in the short wavelength NIR region of the spectrum. As can be seen in Figure 29, this region shows a good similarity to the ORD curve of pure sucrose.

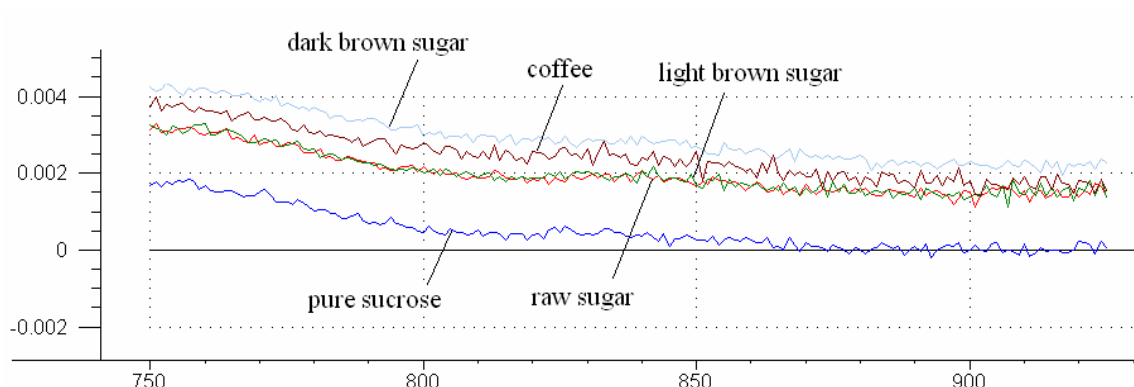


Figure 29. Overlaid spectra of four colored samples of sugar using NIR spectropolarimetry.

Figure 29 shows the ORD curves of the four samples analyzed. These ORD curves all show the same basic shape as that attained with pure sucrose, with no obvious extreme absorption features, opening the possibility to make sugar determinations without the need of previous clarification using lead subacetate. The procedure might be an alternative to other methods for analyses of sugars in other products such as soft drinks and other beverages.^{41, 42, 43, 45}

Another application for determining sucrose is following the kinetics of inversion in acidic medium.^{45, 46, 47} As well as in the measurement of the Pol value, inversion measurements also require clarification. Inversion measurements are important to determine adulteration in honey, quantify the sweetness of a product or simply to

determine total sugars.⁴⁴ Figures 30 and 31 show the results for inversion studies followed polarimetrically and spectropolarimetrically with background correction. Table 4 shows the rate constants calculated by curve fitting using MS-EXCEL solver tool. The procedure for the calculations and other considerations are shown in the Appendix.

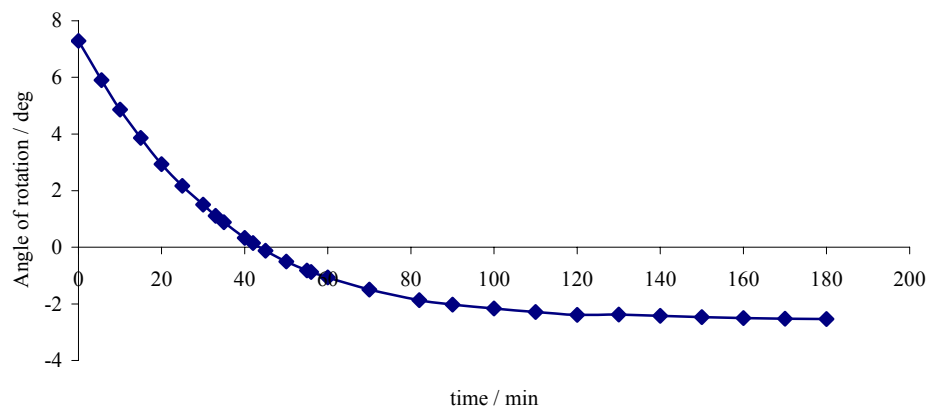


Figure 30. Angle of rotation vs. time for the inversion of sucrose followed polarimetrically at 589 nm.

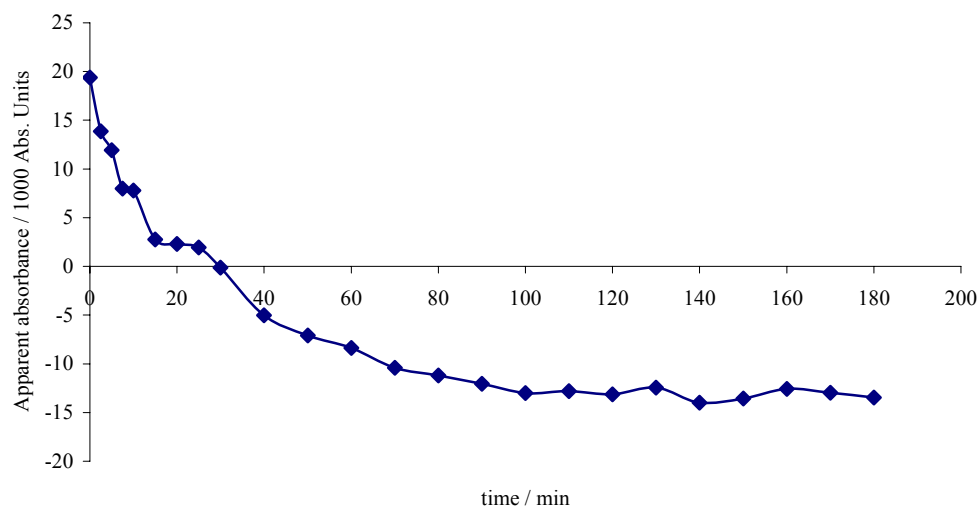


Figure 31. Absorbance vs. time for the inversion of sucrose followed spectropolarimetrically at 589 nm.

Table 4. Values of the rate constants obtained for one colorless sample and one colored sample, by conventional polarimetry and using spectropolarimetry with background correction, respectively.

Sample	Rate constant / min^{-1}
Pure sucrose (polarimetry, 589 nm)	(0.030±0.002)
Pure sucrose (spectropolarimetry, 589 nm)	(0.033±0.008)
Dark brown sugar (spectropolarimetry, 850 nm)	(0.034±0.008)

The inversion of sucrose followed using the new instrument with background correction shows good agreement with polarimetric results. The values of the rate constants are shown in Table 4, and differ approximately 10% from one another. The versatility of the background correction was proven following the rate of inversion with dark brown sugar. The inversion kinetics appears in Figure 32. It was followed at 850 nm because at this wavelength color interferences were minimum compared to other wavelengths. The rate constant calculated is in good agreement with the other results in Table 4.

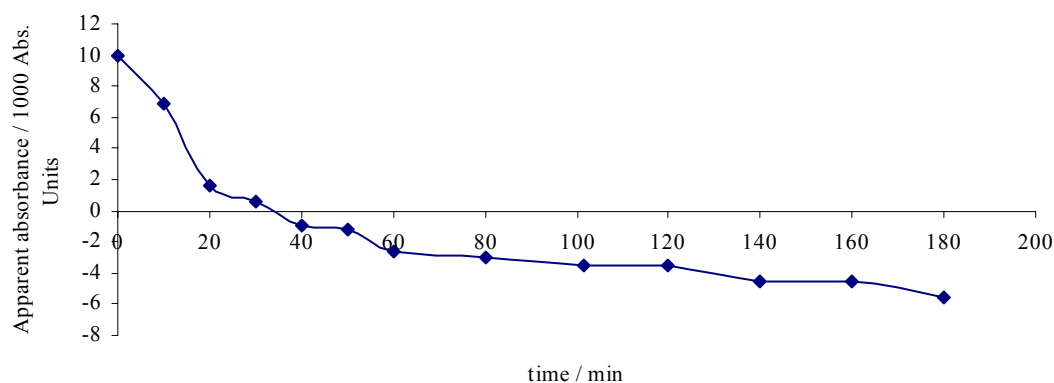


Figure 32. Absorbance vs. time for the inversion of dark brown sugar followed spectropolarimetrically at 850 nm.

Enantiomeric Discrimination

The new spectropolarimeter with background correction was tested also for enantiomeric discrimination. In conventional spectropolarimetry, the ORD curves of a pair of enantiomers are also mirror images of each other because the angles of rotation have the same magnitude but opposite directions. Figure 33 shows a pair of ORD fragments between 350 and 650 nm for (S)-(-)-limonene and (R)-(+)-limonene. As can be seen in Figure 33, both curves have opposite trends, and they converge as they approach 0°, which is the optical rotation of a racemic mixture. Similar plots appear in the appendix for L-arabinose, D-arabinose, (*R,R*)-(+)-*N,N'*-bis(α -methylbenzyl)sulfamide and (*S,S*)-(-)-*N,N'*-bis(α -methylbenzyl)sulfamide.

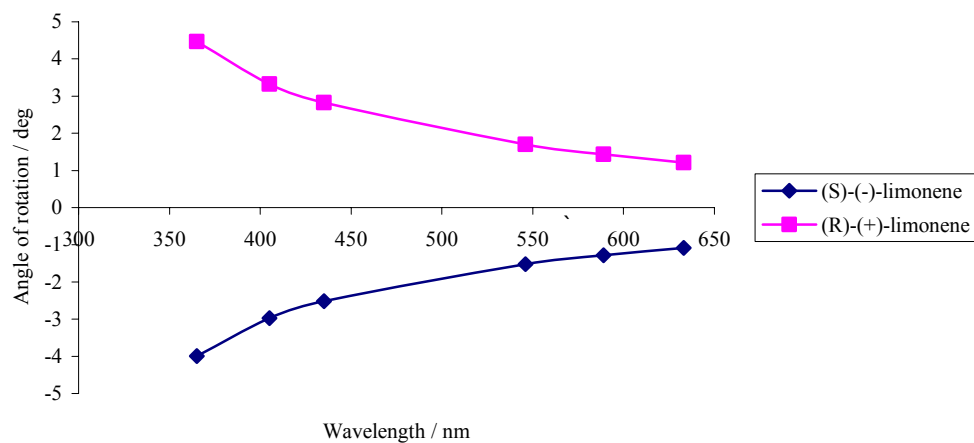


Figure 33. Optical rotatory dispersion for S and R limonene using an Autopol III Polarimeter between 350 and 650 nm.

Since it has been demonstrated that absorbances recorded with the new instrument are equivalent to angles of rotation, the same behavior of opposite curves can be expected from the pseudo-absorption produced using a set of crossed polarizers at a fixed angle. Figure 34 shows this result for limonene. Similar spectra appear in Appendix C for

L-arabinose, D-arabinose, (*R,R*)-(+)-*N,N'*-bis(α -methylbenzyl)sulfamide and (*S,S*)-(-)-*N,N'*-bis(α -methylbenzyl)sulfamide. Figure 34 shows a similar trend as Figure 33. An advantage of this outcome is the possibility of recording absorbances at a continuum of wavelengths. Since these absorbances are related to the presence of a particular chiral compound, it might be possible to build a multivariate regression model based on partial-least-squares regression to predict enantiomeric composition. Figure 35 shows such a model build for limonene. A similar model for arabinose is shown in Appendix C.

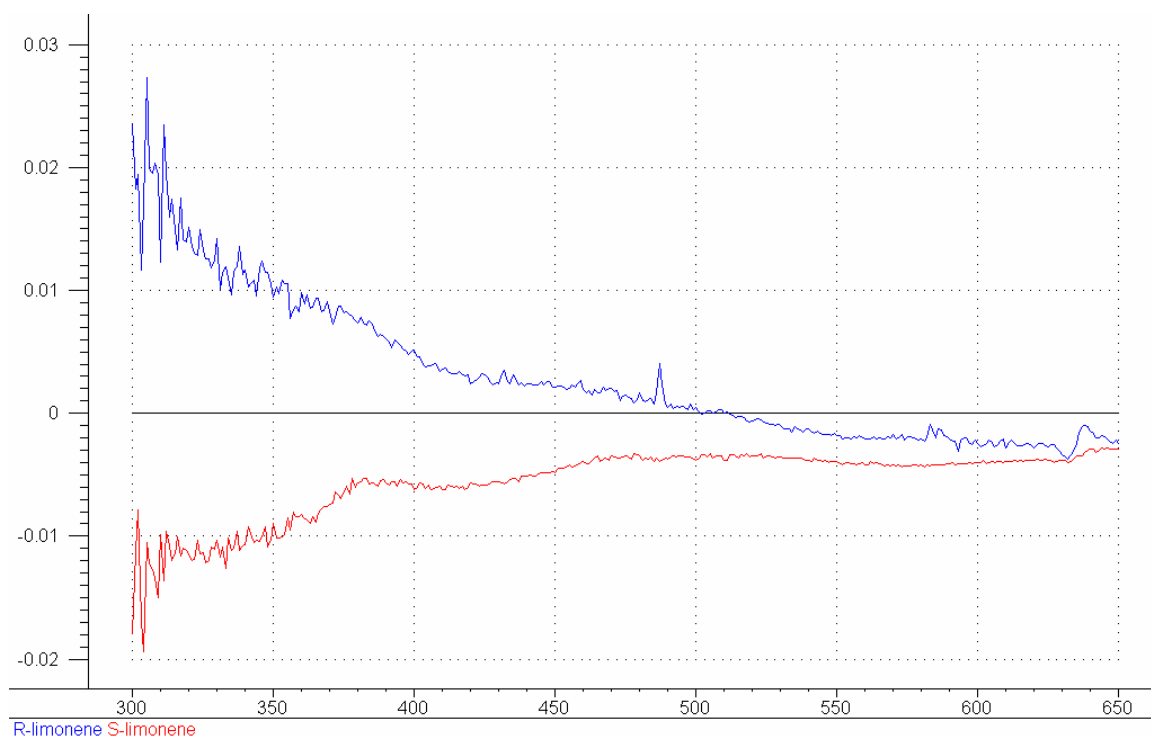


Figure 34. Optical rotatory dispersion spectra for S and R limonene recorded using a set of crossed polarizers fixed at 45 degrees from one another.

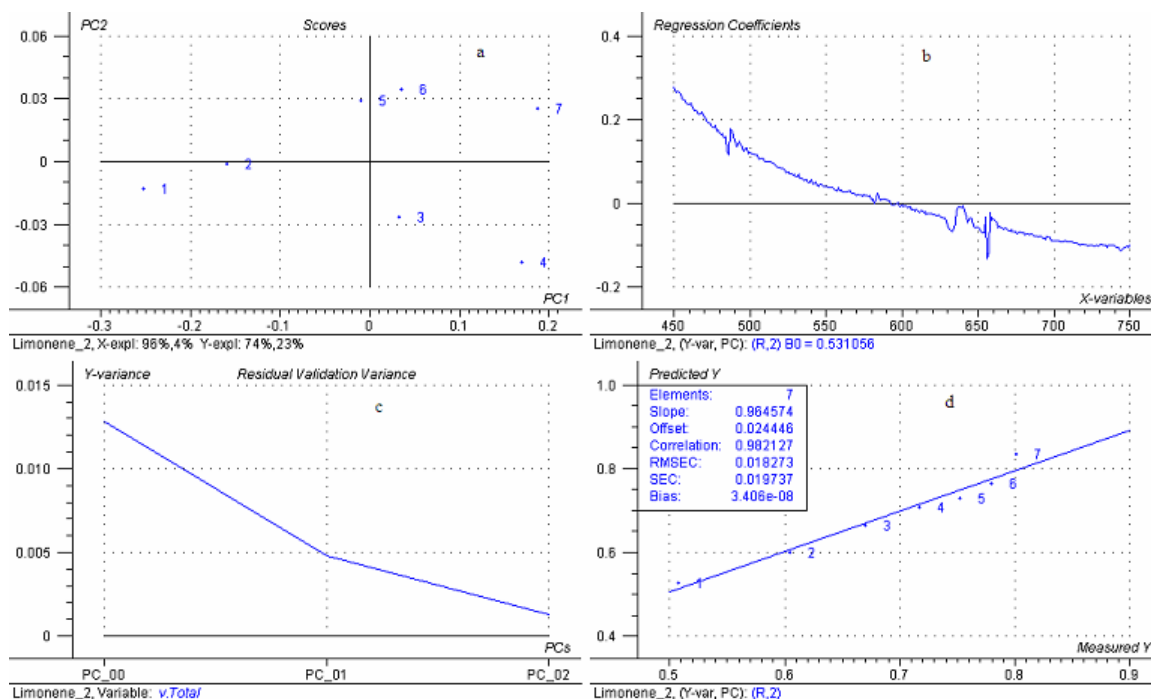


Figure 35. PLS1 model used to predict %R in a mixture of enantiomers for limonene.

The plot of predicted %R versus known %R (Figure 35.d) shows good linearity with a correlation of 0.9821. Figure 35.c shows how two principal components are enough to explain most of the variance of the model. In the case of the absorbances due to optical rotation (X), the first PLS explains 96% of the variation and the second one 4%. With respect to enantiomeric composition (Y), the first PLS component explains 74% of the variation and the second one 23%. In both cases, the fact that the variance decreases largely from the first PLS component to the second one, and that only two PLS components are required, are evidence of the reliability of this model.

The regression coefficients plot (Figure 35.b) is similar to that shown in Figure 27.b, in the sense that it confirms that the absorbance values recorded with background correction isolate the pseudo-absorbance due to rotation from other extraneous absorbances (for example, that from solute-solvent interactions). In this case, the solvent

was methanol, which apparently does not show any interference because of possible absorptions in the region of application of the model. The scores plot (Figure 35.a) shows that the samples are independent from each other, i.e. all have different %R.

Table 5. Results of the prediction of enantiomeric composition expressed as % of (R)-(+)-limonene, using PLS1 between 450 and 750 nm.

Sample	Reference %R	Predicted %R	% Error
1	50.7	52.8	4.14
2	60.5	59.9	-1.00
3	67.0	66.5	-0.75
4	71.7	70.8	-1.26
5	75.2	73.1	-2.79
6	77.9	76.5	-1.80
7	80.1	83.5	4.24

Table 5 shows the results of the prediction based on the model shown in Figure 35, applied to another independent set of seven samples. The reference values correspond to those obtained from the preparation of the solutions. As can be seen all predictions are in good agreement with the reference %R. This results suggest an alternative method to determine enantiomeric composition, to those currently available using HPLC with polarimetric detection^{48,49,50,51,52} or photometric detection.^{53,54,55,56} Figure 36 shows a complementary model based on % S. It has the same characteristics as Figure 35, but the regression coefficients plot (Figure 36.b) and the scores plot (Figure 36.a), reflect opposite behaviors. This is a consequence of opposite ORD spectra for the enantiomeric pair, so that not only the ORD's are opposite but also the regression coefficients have opposite signs. Prediction results appear in Table 6 and are in good agreement with the results for % R in Table 5.

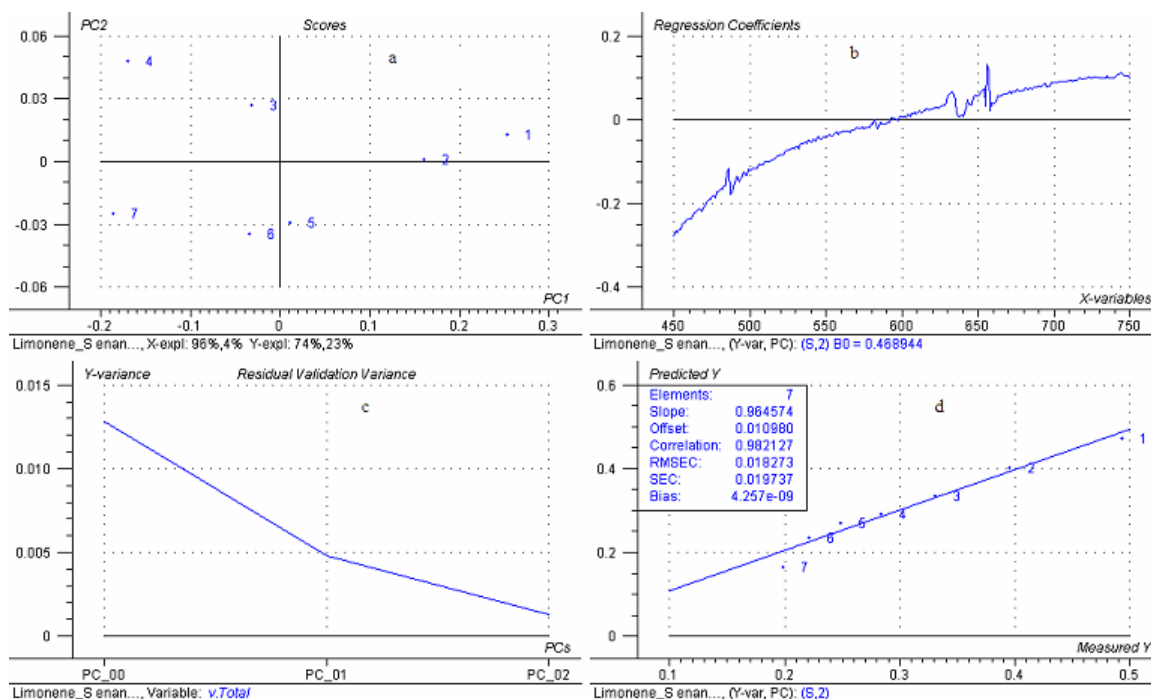


Figure 36. PLS1 model used to predict %S in a mixture of enantiomers for limonene.

Table 6. Results of the prediction of enantiomeric composition expressed as % of (S)-(-)-limonene, using PLS1 between 450 and 750 nm.

Sample	Reference %S	Predicted %S	% Error
1	49.3	47.2	-4.26
2	39.5	40.1	1.52
3	33.0	33.5	1.52
4	28.3	29.2	3.18
5	24.8	26.9	8.47
6	22.1	23.5	6.33
7	19.9	16.5	-17.1

Another important observation is the possibility of determining enantiomeric composition when the total concentration is changing. Enantiomeric composition has been determined with multivariate regression by keeping total concentration constant and changing the molar fraction of each enantiomer. However, no study had been made by varying the total concentration and molar fraction simultaneously. Figure 37 shows a model similar to that in Figure 35. The calibration set used was the same, but instead of

determining % R, it was tested for total concentration of limonene. The results are similar for the model to determine % R and has an increased linearity. The results on a validation model are shown in Table 7, and agree with the reference values.

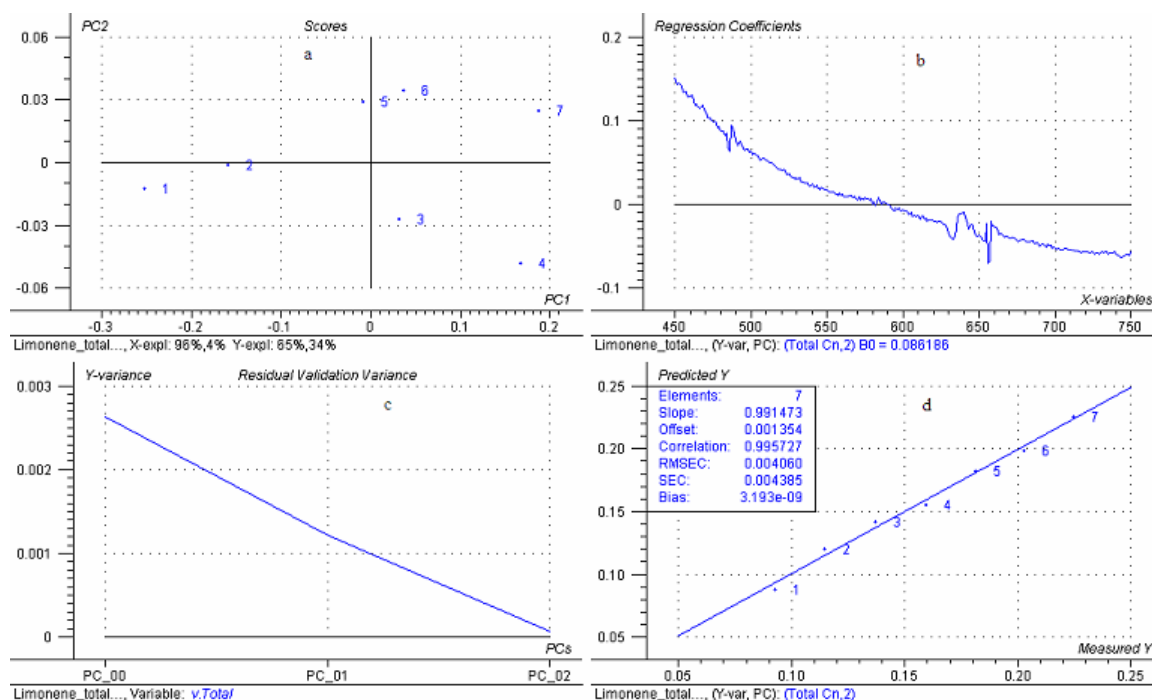


Figure 37. PLS1 model used to predict total concentration of limonene in a mixture of enantiomers.

Table 7. Prediction of total concentration of limonene using PLS1 between 450 nm and 750 nm.

Sample	Reference Cn /mol/L	Predicted Cn /mol/L	% Error
1	0.0925	0.0877	-5.19
2	0.115	0.120	4.35
3	0.137	0.142	3.65
4	0.159	0.156	-1.89
5	0.181	0.183	1.10
6	0.203	0.198	-2.46
7	0.224	0.225	0.45

CHAPTER SIX

Conclusions

As shown previously, the instrument described in this thesis behaves as a spectropolarimeter. Absorbance values recorded using crossed polarizers at a fixed angle of 45 degrees, have been shown to be equivalent to angle of rotation measurements. Therefore, the pseudo absorption spectrum represents an ORD curve based on a transformation given by the Law of Malus.

The instrument was tested successfully for determination of sucrose. The results show that no clarification using lead sub acetate was necessary when using background correction with the sample as its own blank combined with multivariate linear regression. The background correction is achieved by a simple displacement of the cell without introducing additional error in the analysis. Furthermore, using each sample as its own blank permits the isolation of the pseudo absorbance due to rotation from any other absorbances that might be present in solution. Important evidence for this observation is the result that shows that when using the solution as its own blank, the partial least squares regression gives better predictions than when water is used as a blank.

Inversion of sucrose proved to be feasible with both colorless and colored sugars. Both constitute important results for the sugar industry, providing a near infrared spectropolarimeter with no moving parts, that can be calibrated to give % Pol and Brix content.

The instrument also proved to be versatile for enantiomeric discrimination and quantification of the enantiomeric excess, independently of the solvent used. It can be concluded that a spectropolarimetric arrangement of crossed polarizers at a fixed angle of 45 degrees is a good chiroptical technique. When used over a range of wavelengths, the resulting plot is an ORD curve that can be used to study chiral samples with little or no absorption in the UV-vis region because of the absence of chromophores in their structures. Enantiomeric excess was successfully quantified by multivariate linear regression for limonene. The regression parameters specified in the regression output confirm good linearity and a high level of prediction ability based on partial least squares regression on the optical rotatory dispersion curves of limonene.

The proposed configuration has several advantages that make the instrument very attractive. It has no moving parts, the polarizers are fixed, so no modulation is necessary. It has a solid state array detection that provides a wavelength coverage from 200-1100 nm and a stable wavelength axis. Since it is working as a spectropolarimeter, it gives the same results with optical rotation encoded as absorbance. Because absorbances are additive, background correction to remove absorption by colored achiral sample components avoids the necessity of chemical pretreatment, therefore, simplifying sample preparation. Additional advantages are: a stable absorbance axis permits reliable detection of very small absorbance differences, a large sample compartment to accommodate long cells, and multiwavelength data collection permits use of multivariate regression modeling in calibration.

APPENDIX

APPENDIX

Other Models Tested To Predict Sucrose Concentrations

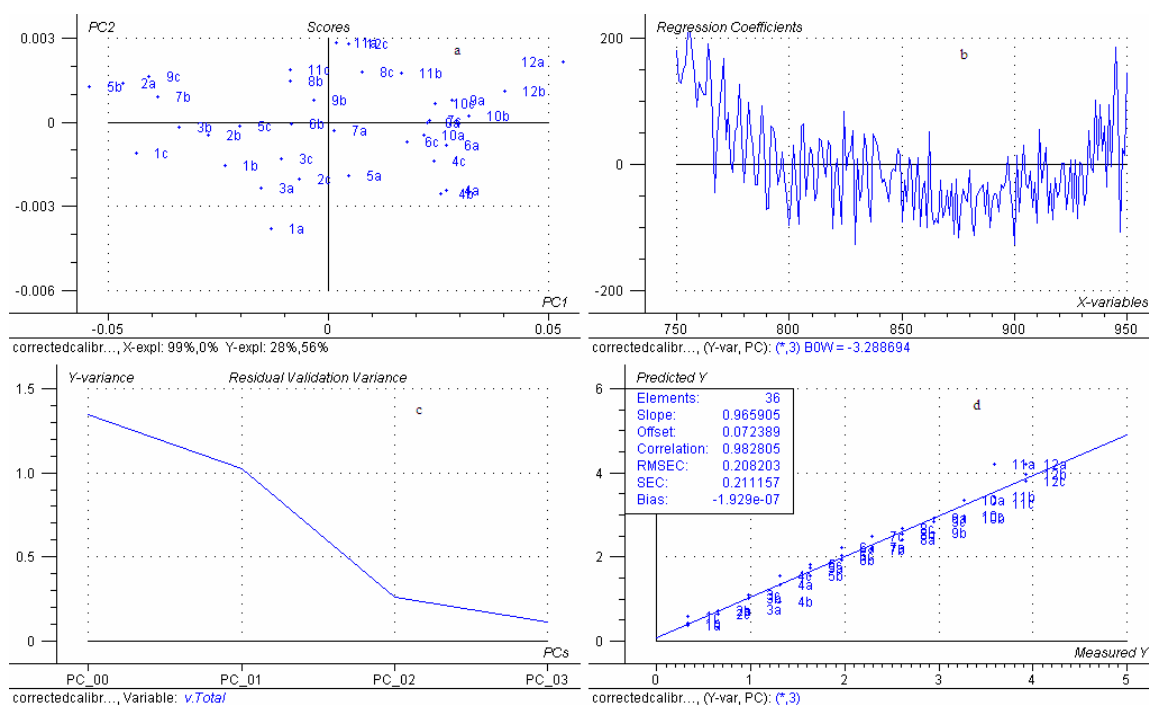


Figure A.1. PLS1 model using 36 samples of colorless sucrose solutions between 750 and 950 nm.

The model shown in Figure A.1 is based on a calibration set of 36 samples measured with background correction. Although the model has good linearity (Figure A.1.d) and shows independency among the samples (Figure A.1.a), it has an irregular behavior in the variance of the predicted concentrations. Figure A.1.c shows that 99% of the variance of the absorbances (X) is explained by the model; however, the first PLS component explains only 28% of the predicted concentrations, and the second PLS component explains 56%, which is opposite to what is expected for PLS regression. As the number

of PLS components necessary to explain the variance of the data, the model is less reliable for prediction. A third PLS component is shown at the bottom of Figure A.1.c. Figure A.1.b shows a regression coefficients plot that might be related to the need for more than two PLS components to obtain reliable predictions.

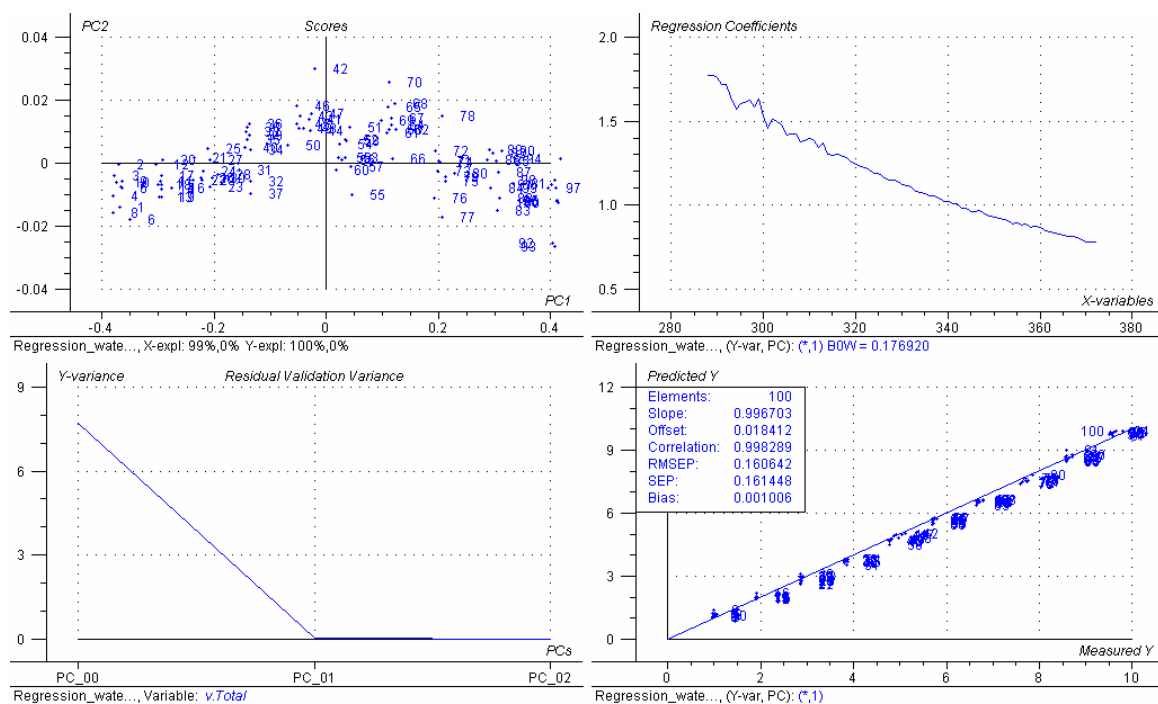


Figure A.2. Model using water blank for 100 samples of colorless sucrose solutions between 282 and 372 nm.

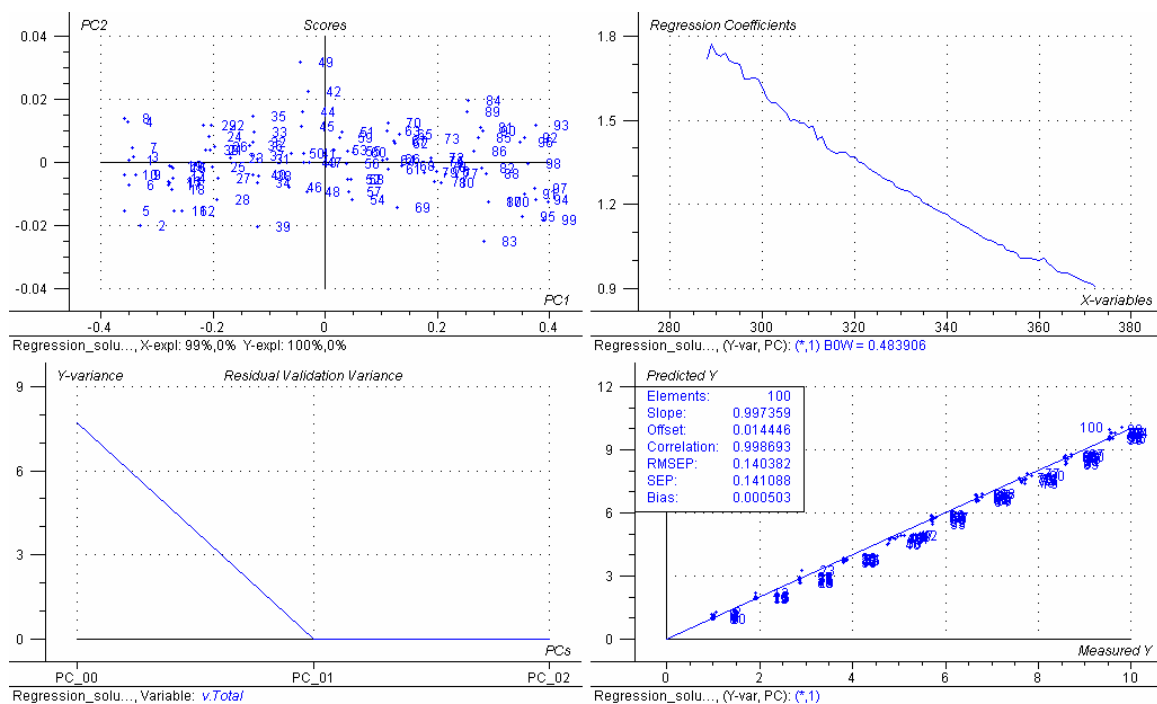


Figure A.3. Model with background correction for 100 samples of colorless sucrose solutions between 282 and 372 nm.

Table A.1. Results obtained with the models shown in Figures A.2 and A.3.

Sample	Reference % w/w	Polarimetric % w/w	% Error	Spectropolarimetric % w/w between 280 nm - 380 nm without background correction	% Error	Spectropolarimetric % w/w between 280 nm - 380 nm with background correction	% Error
1	1.92	1.98	3.13	1.54	-19.8	1.82	-5.21
2	1.93	1.92	-0.52	1.69	-12.4	1.80	-6.74
3	1.92	1.91	-0.52	1.78	-7.29	1.62	-15.6
4	3.8	3.69	-2.89	3.53	-7.11	3.62	-4.74
5	3.81	3.74	-1.84	3.6	-5.51	3.71	-2.62
6	3.82	3.75	-1.83	3.61	-5.50	3.81	-0.26
7	5.73	5.66	-1.22	5.68	-0.87	5.83	1.75
8	5.73	5.67	-1.05	5.47	-4.54	5.52	-3.66
9	5.73	5.65	-1.40	5.72	-0.17	5.59	-2.44

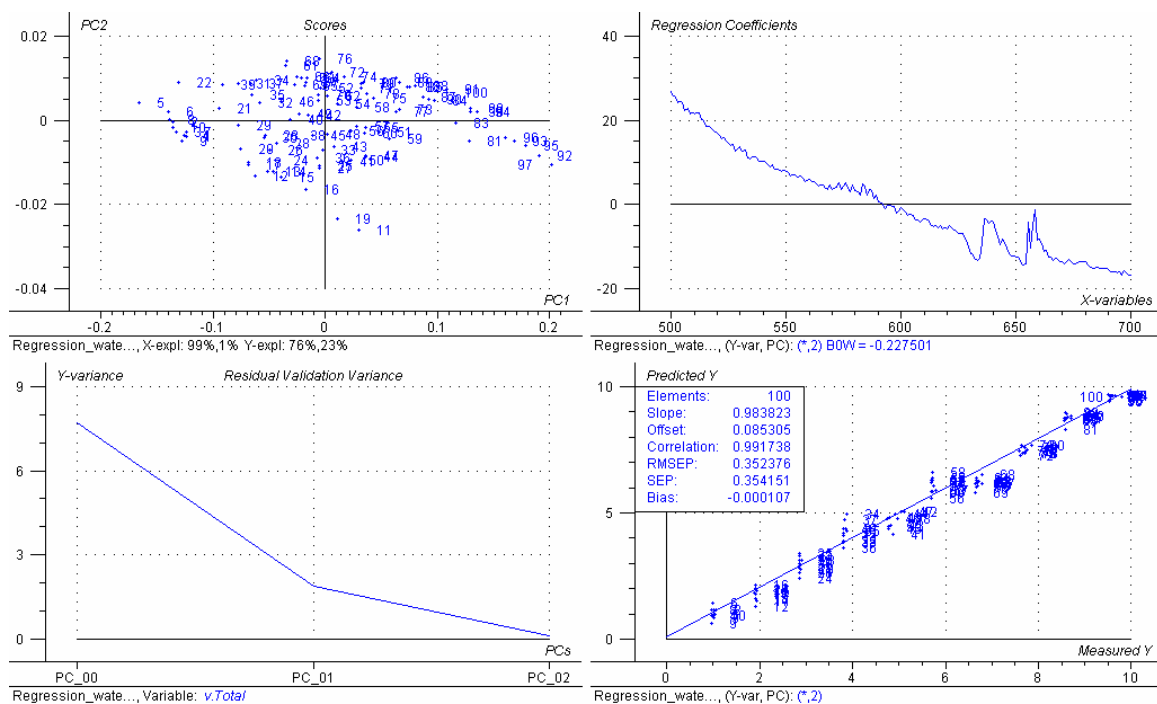


Figure A.4. Model using water blank for 100 samples of colorless sucrose solutions between 500 and 700 nm.

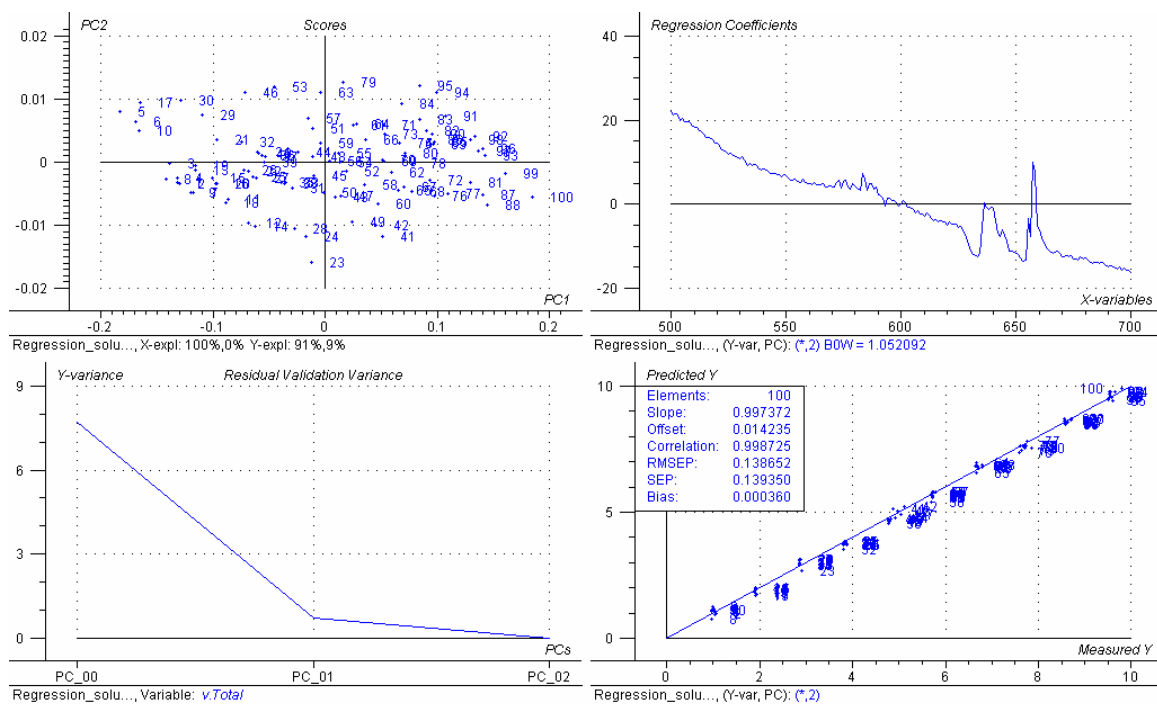


Figure A.5. Model with background correction for 100 samples of colorless sucrose solutions between 500 and 700 nm

Table A.2. Results obtained with the models shown in Figures A.4 and A.5.

Sample	Reference % w/w	Polarimetric % w/w	% Error	Spectropolarimetric % w/w between 500 nm - 700 nm without background correction	% Error	Spectropolarimetric % w/w between 500 nm - 700 nm with background correction	% Error
1	1.92	1.98	3.13	1.89	-1.56	1.79	-6.77
2	1.93	1.92	-0.52	1.75	-9.33	2.32	20.2
3	1.92	1.91	-0.52	1.68	-12.5	1.89	-1.56
4	3.8	3.69	-2.89	3.63	-4.47	3.62	-4.74
5	3.81	3.74	-1.84	4.55	19.4	3.83	0.52
6	3.82	3.75	-1.83	4.41	15.4	3.86	1.05
7	5.73	5.66	-1.22	6.04	5.41	5.91	3.14
8	5.73	5.67	-1.05	6.45	12.6	5.55	-3.14
9	5.73	5.65	-1.40	6.40	11.7	5.52	-3.66

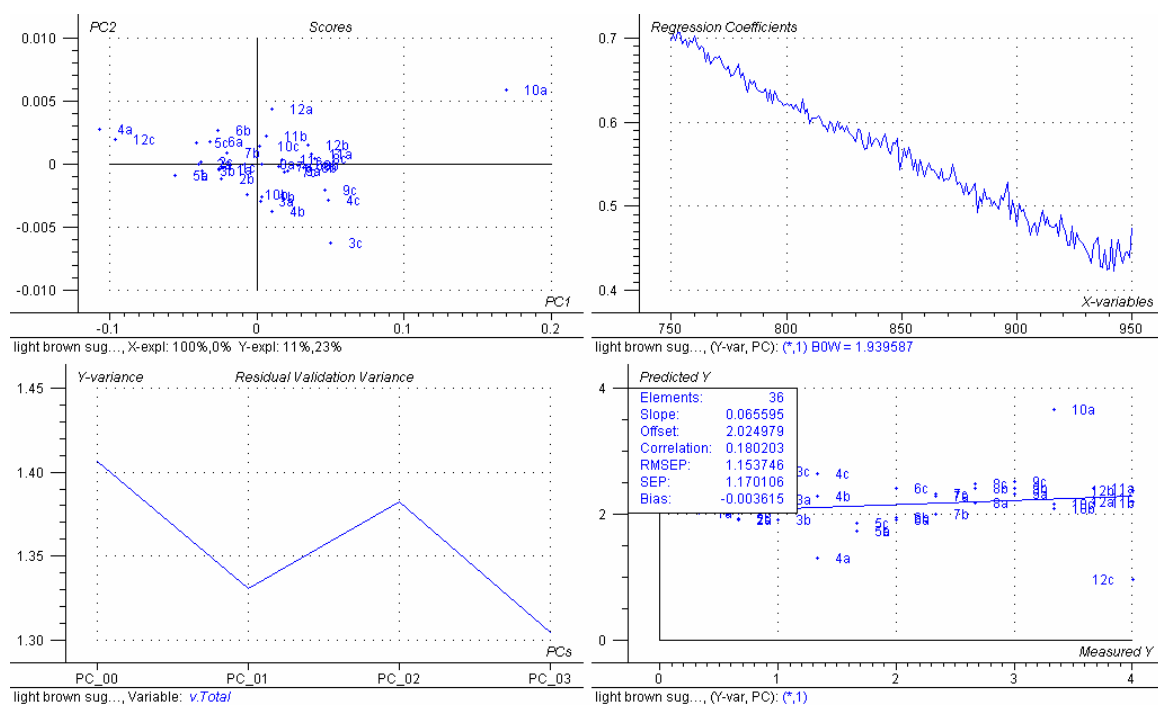


Figure A.6. Model using background correction for light brown sugar solutions between 750 and 950 nm.

Spectropolarimetric Determination of Sucrose Inversion Using Absorbance Measurements

Another type of measurement done routinely in the sugar industry is to follow the inversion of sucrose, which is also affected by the presence of color. Sucrose inversion is the hydrolysis of sucrose in acidic medium into its constituent monosaccharides glucose and fructose (inverted sugar is of special interest due to its increased sweetness over ordinary sucrose). Because of the differences in optical activities of the latter compounds with respect to sucrose, the rate of inversion can also be followed polarimetrically. A general polarimetric procedure is explained by Daniels. For the particular case of the set-up presented in this work, sucrose inversion is followed spectrophotometrically.

Sucrose is a disaccharide that undergoes hydrolysis in acidic medium. The products of the hydrolysis are the monosaccharides glucose and fructose. This process is known as inversion. The rate law for the inversion of sucrose is:

$$d[\text{sucrose}]/dt = k [\text{sucrose}]^m [\text{H}_2\text{O}]^n [\text{H}^+]^p \quad (\text{A.1})$$

From Equation A.1 it can be seen that the rate of inversion depends on the concentration of sucrose, water and acid. The concentration of water and acid are essentially constant. So Equation A.1 can be rewritten to specify the dependence on the concentration of sucrose only:

$$-d[\text{sucrose}]/dt = k_{\text{eff}} [\text{sucrose}]^m \quad (\text{A.2})$$

where

$$k_{\text{eff}} = k [\text{H}_2\text{O}]^n [\text{H}^+]^p \quad (\text{A.3})$$

The experimental conditions require water to be in excess and the acid in a concentration equal to 4 *M*. Under such conditions it can be assumed that the reaction is

pseudo first order in sucrose, $m=1$, which is verified fitting experimental data to a first-order integrated rate law. In the equations that follow, $[\text{sucrose}] = c$. It is also assumed that the reaction goes to completion so that practically no sucrose remains at "infinite" time. The integrated form of the pseudo first-order-reaction differential equation is then:

$$c = c_0 e^{-k_{\text{eff}} t} \quad (\text{A.4})$$

where c_0 is the concentration of sucrose at the beginning of the reaction. Taking logarithms,

$$\ln(c/c_0) = -kt \quad (\text{A.5})$$

Thus the slope of a plot of $\ln c/c_0$ versus t is $-k$. However, in this experiment the concentration of sucrose is not directly measured. Instead absorbance, Abs , is measured. Absorbance is directly proportional to concentration. Using the crossed polarizers set-up, the inversion of sucrose is followed in a similar way to that in which this process is followed polarimetrically. For an optically active molecule in solution, the crossed polarizers set-up allows the measurement of absorbance as an equivalent of the angle of rotation:

$$Abs_i = \xi_i c_i \quad (\text{A.6})$$

for ξ_i a constant dependent on the molecule i . For a solution of sucrose, glucose, and fructose:

$$Abs = \xi_{\text{sucrose}} c_{\text{sucrose}} + \xi_{\text{glucose}} c_{\text{glucose}} + \xi_{\text{fructose}} c_{\text{fructose}} \quad (\text{A.7})$$

At the end of the reaction, no sucrose remains and:

$$Abs_{\infty} = \xi_{\text{glucose}} c_{\text{glucose},\infty} + \xi_{\text{fructose}} c_{\text{fructose},\infty} \quad (\text{A.8})$$

From the stoichiometry,

$$c_{\text{glucose},\infty} = c_{\text{fructose},\infty} = c_{\text{sucrose},0} \quad (\text{A.9})$$

where $c_{\text{sucrose},0}$ is the initial concentration of sucrose. Substituting Equation A.9 in to Equation A.8 gives:

$$Abs_{\infty} = (\xi_{\text{glucose}} + \xi_{\text{fructose}}) c_{\text{sucrose},0} \quad (\text{A.10})$$

At the beginning of the reaction:

$$Abs_0 = \xi_{\text{sucrose}} c_{\text{sucrose},0} \quad (\text{A.11})$$

Subtracting Equation A.10 from Equation A.11 gives:

$$Abs_0 - Abs_{\infty} = (\xi_{\text{sucrose}} - \xi_{\text{glucose}} - \xi_{\text{fructose}}) c_{\text{sucrose},0} \quad (\text{A.12})$$

During the course of the reaction at time t:

$$Abs_t = \xi_{\text{sucrose}} c_{\text{sucrose}} + \xi_{\text{glucose}} c_{\text{glucose}} + \xi_{\text{fructose}} c_{\text{fructose}} \quad (\text{A.13})$$

However, from the 1:1 stoichiometry and Equation A.9

$$c_{\text{glucose}} = c_{\text{fructose}} = c_{\text{sucrose},0} - c_{\text{sucrose}} \quad (\text{A.14})$$

which when substituted into Equation A.13 and then Equation A.10 is subtracted gives:

$$Abs_t - Abs_{\infty} = \xi_{\text{sucrose}} c_{\text{sucrose}} - \xi_{\text{glucose}} c_{\text{sucrose}} - \xi_{\text{fructose}} c_{\text{sucrose}} \quad (\text{A.15})$$

or grouping terms:

$$Abs_t - Abs_{\infty} = (\xi_{\text{sucrose}} - \xi_{\text{glucose}} - \xi_{\text{fructose}}) c_{\text{sucrose}} \quad (\text{A.16})$$

Dividing Equation A.16 by Equation A.12 then gives the desired concentration ratio:

$$(Abs_t - Abs_{\infty}) / (Abs_0 - Abs_{\infty}) = c_{\text{sucrose}} / c_{\text{sucrose},0} \quad (\text{A.17})$$

Finally substituting Equation A.17 into Equation A.4 gives:

$$(Abs_t - Abs_{\infty}) = (Abs_0 - Abs_{\infty}) e^{-k_{\text{eff}} t} \quad (\text{A.18})$$

or

$$Abs_t = (Abs_0 - Abs_{\infty}) e^{-k_{\text{eff}} t} + Abs_{\infty} \quad (\text{A.19})$$

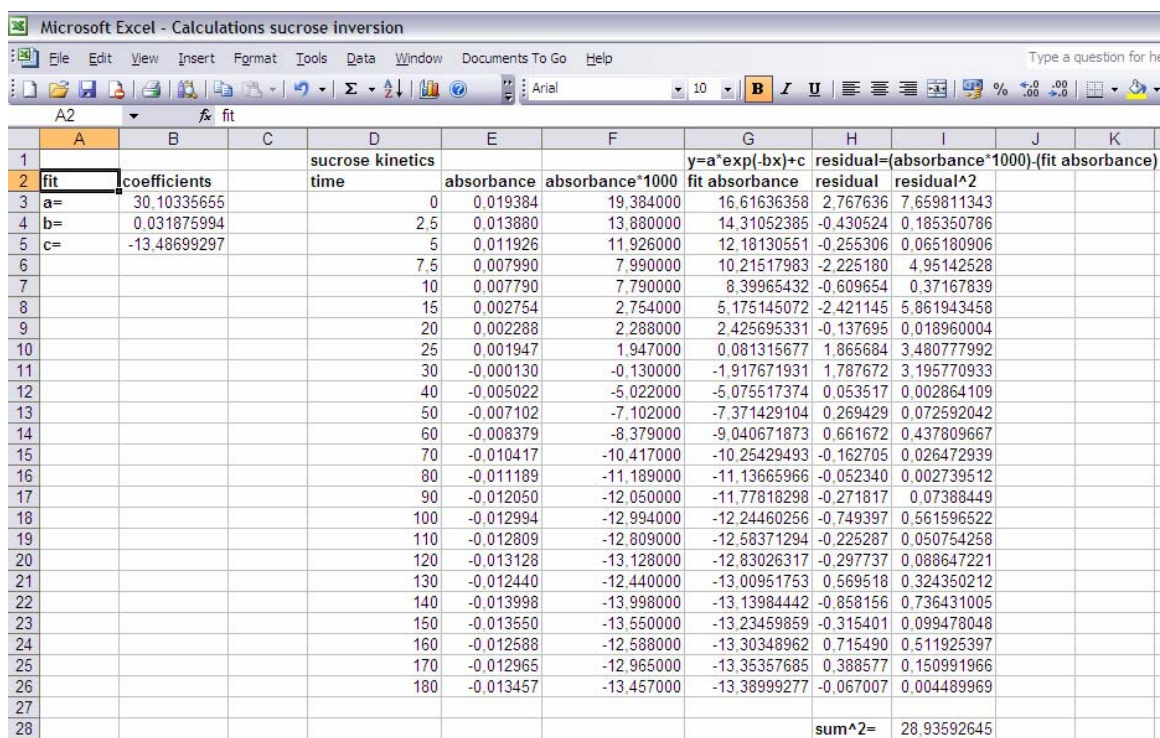
Substituting Equation A.17 into Equation A.5 gives

$$\ln[(Abs_t - Abs_{\infty}) / (Abs_0 - Abs_{\infty})] = -k t \quad (\text{A.20})$$

or

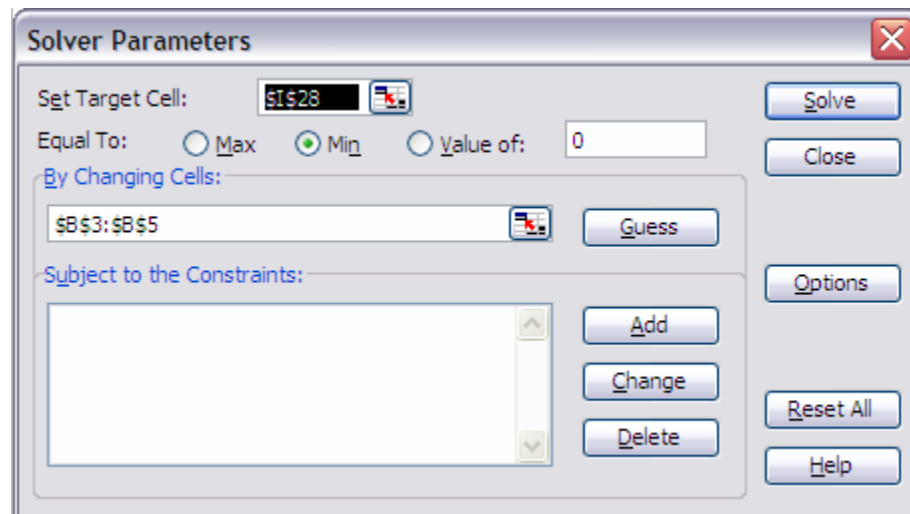
$$\ln(Abs_t - Abs_{\infty}) = -kt + \ln(Abs_0 - Abs_{\infty}) \quad (A.21)$$

The slope is the same as it would be if actual concentrations had been plotted, or if the recorded data have been angle of rotation measurements. An alternative method to fit data is using the tool *Solver* in *MS-EXCEL* which was used in this work for practical reasons.

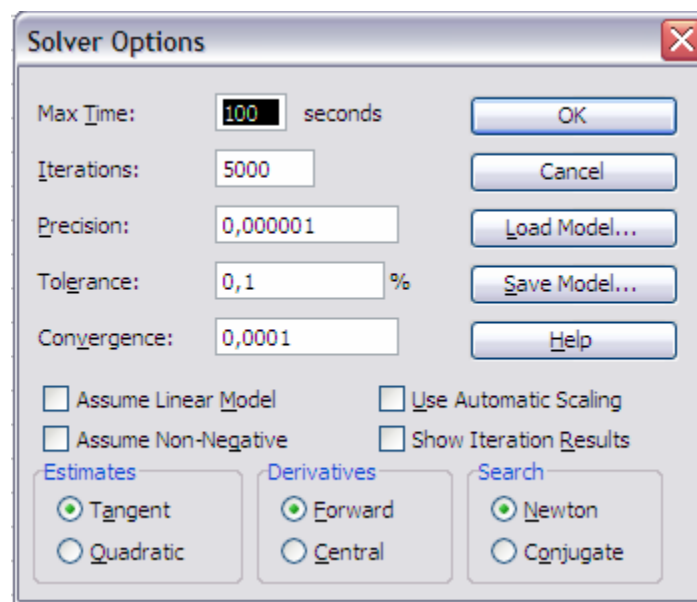


	A	B	C	D	E	F	G	H	I	J	K
				sucrose kinetics	absorbance	absorbance*1000	y=a*exp(-bx)+c	residual=(absorbance*1000)-(fit absorbance)	residual^2		
2	fit	coefficients		time			fit absorbance				
3	a=	30.10335655		0	0.019384	19.384000	16.61636358	2.767636	7.659811343		
4	b=	0.031875994		2.5	0.013880	13.880000	14.31052385	-0.430524	0.185350786		
5	c=	-13.48699297		5	0.011926	11.926000	12.18130551	-0.255306	0.065180906		
6				7.5	0.007990	7.990000	10.21517983	-2.225180	4.95142528		
7				10	0.007790	7.790000	8.39965432	-0.609654	0.37167839		
8				15	0.002754	2.754000	5.175145072	-2.421145	5.861943458		
9				20	0.002288	2.288000	2.425695331	-0.137695	0.018960004		
10				25	0.001947	1.947000	0.081315677	1.865684	3.480777992		
11				30	-0.000130	-0.130000	-1.917671931	1.787672	3.195770933		
12				40	-0.005022	-5.022000	-5.075517374	0.053517	0.002864109		
13				50	-0.007102	-7.102000	-7.371429104	0.269429	0.072592042		
14				60	-0.008379	-8.379000	-9.040671873	0.661672	0.437809667		
15				70	-0.010417	-10.417000	-10.25429493	-0.162705	0.026472939		
16				80	-0.011189	-11.189000	-11.13665966	-0.052340	0.002739512		
17				90	-0.012050	-12.050000	-11.77818298	-0.271817	0.07388449		
18				100	-0.012994	-12.994000	-12.24460256	-0.749397	0.561596522		
19				110	-0.012809	-12.809000	-12.58371294	-0.225287	0.050754258		
20				120	-0.013128	-13.128000	-12.83026317	-0.297737	0.088647221		
21				130	-0.012440	-12.440000	-13.00951753	0.569518	0.324350212		
22				140	-0.013998	-13.998000	-13.13984442	-0.858156	0.736431005		
23				150	-0.013550	-13.550000	-13.23459859	-0.315401	0.099478048		
24				160	-0.012588	-12.588000	-13.30348962	0.715490	0.511925397		
25				170	-0.012965	-12.965000	-13.35357685	0.388577	0.150991966		
26				180	-0.013457	-13.457000	-13.38999277	-0.067007	0.004489969		
27											
28								sum^2=	28.93592645		

Figure A.7. MS-Excel worksheet to determine the rate constant by curve fitting using the solver tool.



a.



b.

Figure A.8. a. MS-Excel solver parameters for curve fitting of inversion data, and b. solver options to assess curve fitting.

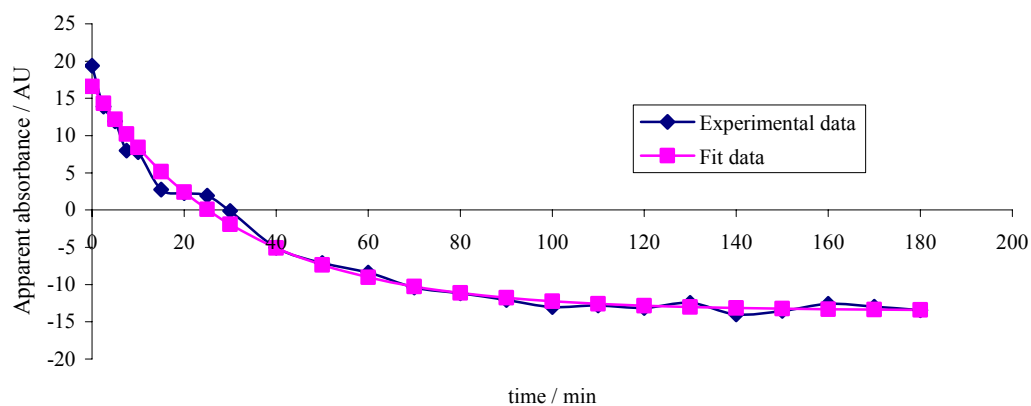


Figure A.9. Overlaid plot of the experimental and fit data for sucrose inversion followed by absorbance measurements using a spectropolarimetric arrangement of fixed crossed polarizers.

Additional Results on Enantiomeric Discrimination

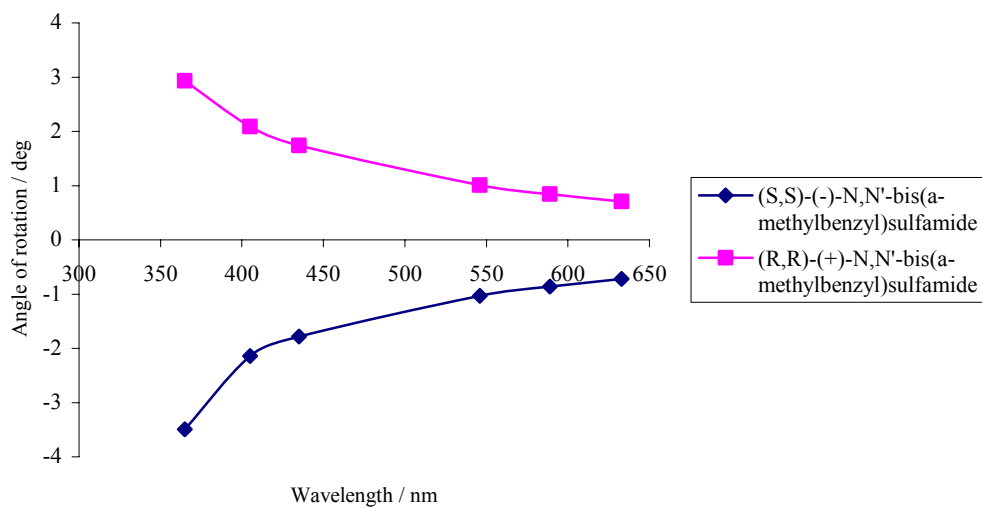


Figure A.10. Optical rotatory dispersion for *(S,S)*-(-)-*N,N'*-bis(a-methylbenzyl)sulfamide and *(R,R)*-(+)-*N,N'*-bis(a-methylbenzyl)sulfamide using an Autopol III Polarimeter between 350 and 650 nm.

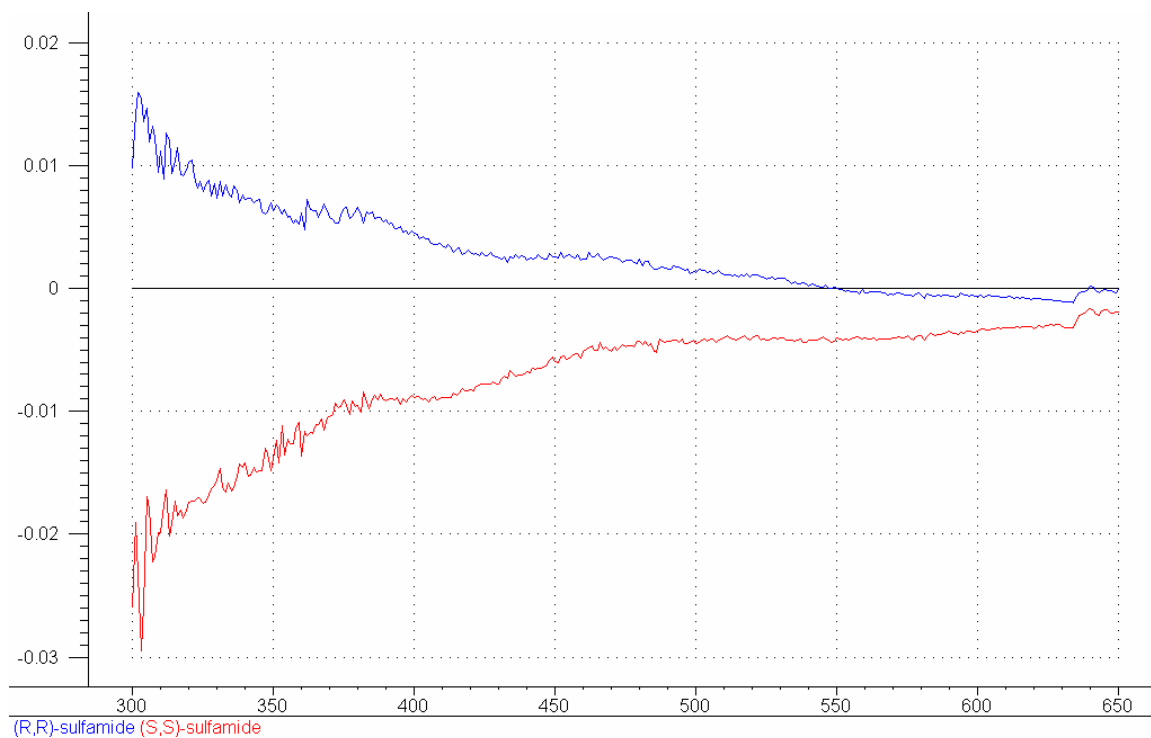


Figure A.11. Optical rotatory dispersion for (S,S) -(-)- N,N' -bis(α -methylbenzyl)sulfamide and (R,R) -(+)- N,N' -bis(α -methylbenzyl)sulfamide using a set of crossed polarizers fixed at 45 degrees from one another.

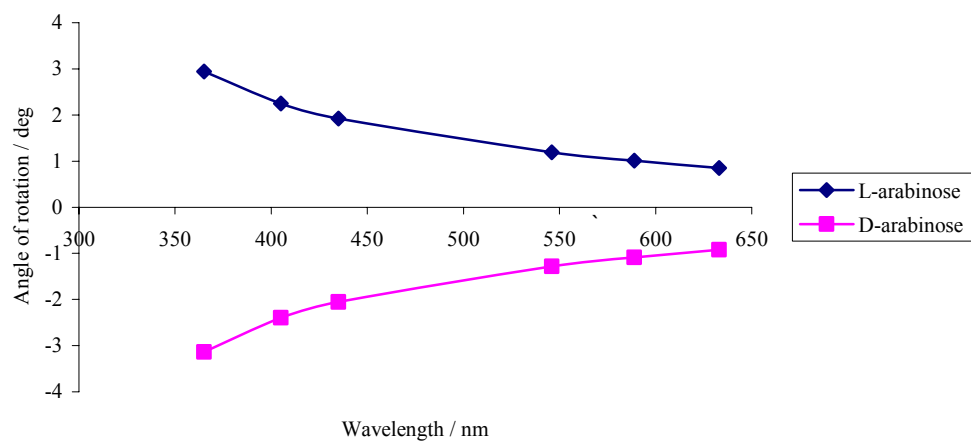


Figure A.12. Optical rotatory dispersion for L-arabinose and D-arabinose using an Autopol III Polarimeter between 350 and 650 nm.

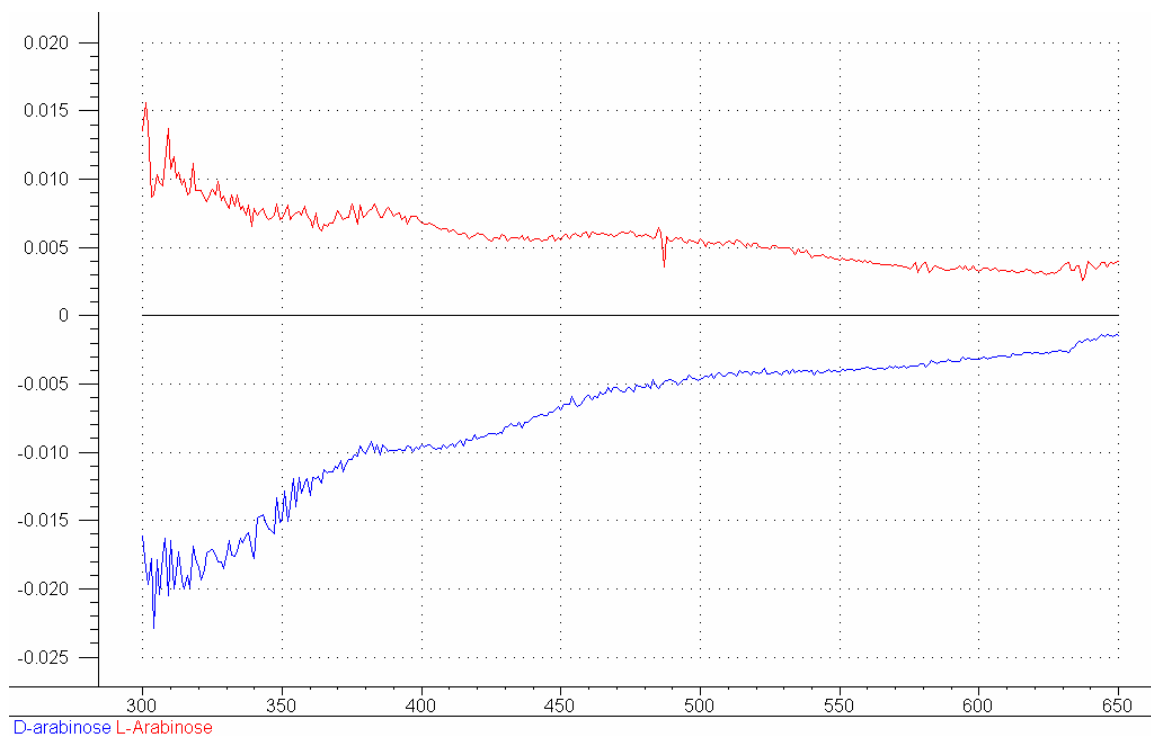


Figure A.13. Optical rotatory dispersion for L-arabinose and D-arabinose using a set of crossed polarizers fixed at 45 degrees from one another.

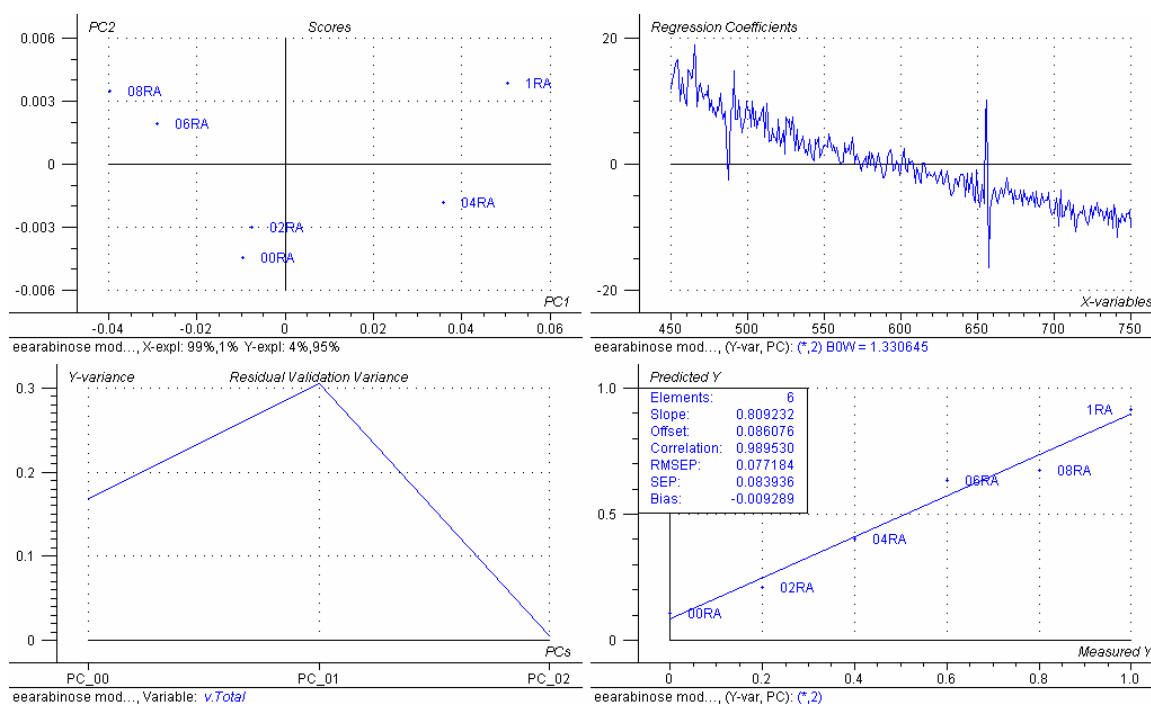


Figure A.14. PLS1 model used to predict %R in a mixture of enantiomers for arabinose.

Spectropolarimetric Configuration

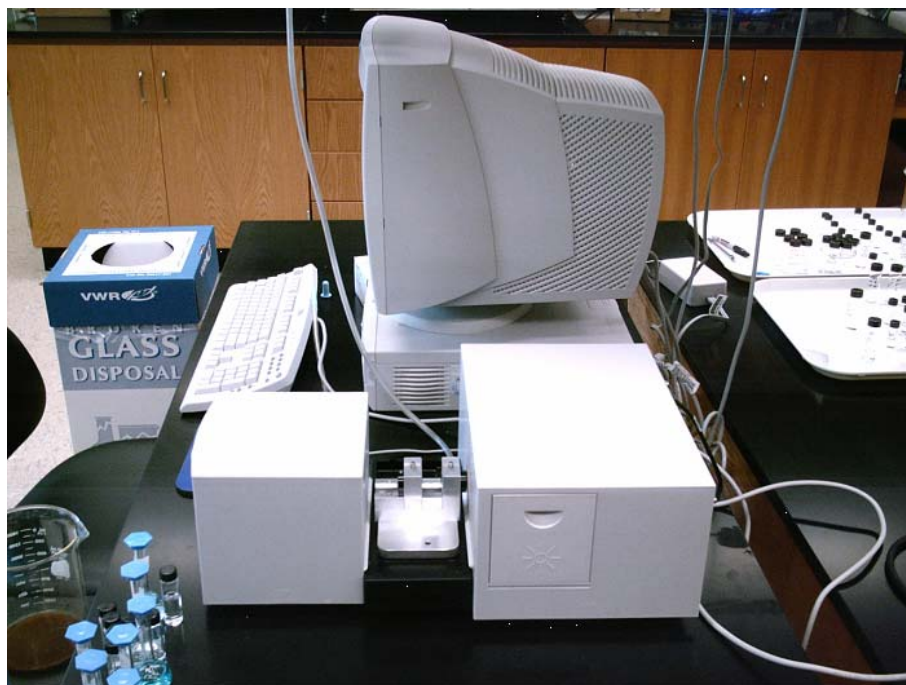


Figure A.15. Spectropolarimetric set-up used in this project.

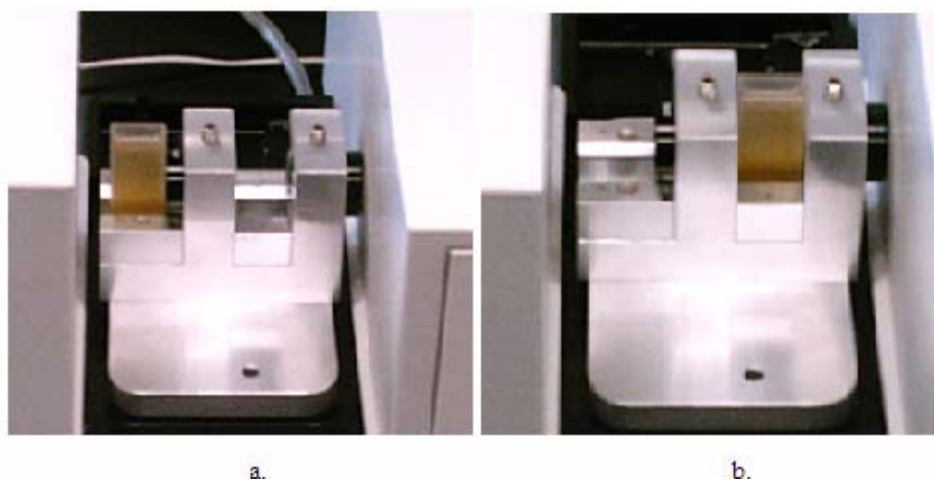


Figure A.16. Relative position of the spectropolarimetric cell for: a. background correction, and b. ORD spectrum recording.

REFERENCES

1. Purdie, N.; Brittain, H. G. *Analytical Applications of Circular Dichroism*; Elsevier: Amsterdam, 1994, pp. 1-90.
2. Busch, K. W.; Busch, M. A.; Calleja-Amador, C. *Instrumental Aspects of Chiroptical Detection*, in *Chiral Analysis*, Busch, K.W. and Busch, M.A. editors. Elsevier, in press.
3. Shurcliff, W. A. *Polarized Light*; Harvard University Press: Cambridge, 1966, pp. 65-77.
4. Collet, E. *Polarized Light, Fundamentals and Applications*; Marcel Dekker Inc.: New York, 1993, pp. 11-19.
5. Robinson, J. W. *Undergraduate Instrumental Analysis*; 5th Ed. Marcel Dekker, Inc.: New York, 1995, pp. 403-408.
6. Snell, F. D.; Ettre, L. S. In *Encyclopedia of Industrial Chemical Analysis*; Interscience Publishers: New York, 1973; Vol. 18, pp. 344-348.
7. Gyura, J. F.; Seres, Z. I.; Beer, A. M. *Acta Periodica Technologica* **2002**, 33, 3.
8. Kuchejda, M.; Ramirez, S.; Yilmaz, S. *Internacional Sugar Journal*. **2005**, 107, 302.
9. Berova, N.; Nakanishi, K.; Woody, R. *Circular Dichroism, Principles and Applications*; John Wiley & Sons: New York, 2000, pp. 1-50, 97-110.
10. Daniels, J. M. *The Review of Scientific Instrumentation* **1967**, 38, 284.
11. Mahurin, S. M.; Compton, R. N.; Zare, R. N. *J. Chem. Educ.* **1999**, 76, 1234.
12. Lloyd, D. K.; Goodall, D. M. *Chirality* **1989**, 1, 251.
13. Voigtman, E. *Anal. Chem.* **1992**, 64, 2590.
14. Brittain, H. G. *Microchemical Journal* **1997**, 57, 137.
15. Engelke, J. *Sugarcane: measuring commercial quality*. Farmnote 23 from the Department of Agriculture: Australia, **2002**.

16. Kishihara, S.; Tamaki, H.; Fujii, S.; Komoto, M. *Journal of Membrane Science* **1989**, *41*, 103.
17. Miyamoto, K.; Kitano, Y. *J. Near Infrared Spectrosc.* **1995**, *3*, 227.
18. Salgó, A.; Nagy, J.; Mikó, É. *J. Near Infrared Spectrosc.* **1998**, *6*, A101.
19. Roggo, Y.; Duponchel, L.; Noe, B.; Huvenne, J. P.; *J. Near Infrared Spectrosc.* **2002**, *10*, 137.
20. Maalouly, J.; Eveleigh, L.; Rutledge, D. N.; Ducauze, C. J. *Vibrational Spectroscopy* **2004**, *36*, 279.
21. Friedemann, T. E.; Weber, C. W.; Witt, N. F. *Analytical Biochemistry* **1963**, *6*, 504.
22. Rambla, F. J.; Garrigues, S.; de la Guardia, M. *Analytica Chimica Acta* **1997**, *344*, 41.
23. Zagatto, E. A. G.; Mattos, I. L.; Jacintho, A. O. *Analytica Chimica Acta* **1998**, *204*, 259.
24. Tewari, J.; Mehrotra, R.; Irudayaraj, J. *J. Near Infrared Spectrosc.* **2003**, *11*, 351.
25. Daniel Kelly, J. F.; Downey, G.; Fouratier, V. *J. Agric. Food Chem.* **2004**, *52*, 33.
26. Schoones, B. M.; Alborough, H. F. *South African Sugar Technologists Association: Abstracts of the 79th Annual Congress.* **2005**, 43.
27. Singleton, V.; Horn, J.; Bucke, C.; Adlard, A. *Journal American Society of Sugarcane Technologies* **2002**, *22*, 112.
28. Brittain, H. G. *J. Pharm. Biomed. Anal.* **1998**, *17*, 933.
29. Agilent Technologies. *Agilent 8453 UV-visible Spectroscopy System: Operator's Manual*: Hewlett-Packard: Germany, 2000, pp. 102.
30. Daniels, F.; Alberty, R. A.; Williams, J. W.; Cornwell, C. D.; Bender, P.; Harriman, J. E. *Experimental Physical Chemistry*. 7th Ed. McGraw – Hill: New York, **1970**, pp. 149-152.
31. Golic, M.; Walsh, K.; Lawson, P. *Appl. Spectrosc.* **2003**, *57*, 139.
32. Hayakawa, K.; Yamamoto, A.; Matsunaga, A.; Mizukami, E.; Nishimura, M.; Miyazaki, M. *Biomedical Chromatography* **1994**, *8*, 130.

33. Pace, N.; Tanford, C.; Davidson, E. A. *J. Am. Chem. Soc.* **1964**, 86, 3160.
34. Yeung, E. S. *Talanta* **1985**, 32, 1097.
35. Kankare, J. J. *Talanta* **1986**, 33, 571.
36. Calleja-Amador, C.; Rabbe, D. H.; Busch, M. A.; Busch, K. W. *A Novel Near Infrared Spectropolarimeter for Determination of Sucrose*. Federation of Analytical Chemistry & Spectroscopy Societies 32nd meeting: Quebec, **2005**, 209.
37. Mark, H.; Workman, K. *Statistics in Spectroscopy*; Academic Press: Boston, **1991**, p. 288.
38. Otto, M. *Chemometrics: Statistics and Computer Application in Analytical Chemistry*; Wiley – VCH: Weinheim, **1999**, pp. 175-207.
39. Morgan, E. *Chemometrics: Experimental Design*; John Wiley & Sons: Chichester, **1995**, pp. 1-53.
40. Wold, S.; Sjostrom, M.; Eriksson, L. *Chemometrics and Intelligent Laboratory Systems* **2001**, 58, 109.
41. Yamamoto, A.; Wataya, T.; Hayakawa, K.; Matsunaga, A.; Nishiruma, M.; Miyazaki, M. *J. Pharm. Biomed. Anal.* **1997**, 15, 1383.
42. Yamamoto, A.; Ohmi, H.; Matsunaga, A.; Mizukami, E.; Ando, K.; Hayakawa, K.; Nishimura, M. *J. Chromatogr. A.* **1998**, 804, 305.
43. Hayakawa, K.; Ando, K.; Yoshida, N.; Yamamoto, A.; Matsunaga, A.; Nishimura, M.; Kitaota, M.; Matsui, K. *Biomedical Chromatography* **2000**, 14, 72.
44. Irudayaraj, J.; Xu, F.; Tewari, J. J. *J. Food Science* **2003**, 68, 2040.
45. Moore, J. W.; Pearson, R. G. *Kinetics and Mechanism*; 3rd Ed. John Wiley & Sons: New York, **1994**, pp. 16-19.
46. Frost, A. A.; Pearson, R.G. *Kinetics and Mechanism*; 2nd Ed. John Wiley & Sons: New York, **1984**, pp. 40-50.
47. Cortes-Figueroa, J. E.; Moore, D. A. *J. Chem. Educ.* **2002**, 79, 1462.
48. Lloyd, D. K.; Goodall, D. M.; Scrivener, H. *Anal. Chem.* **1989**, 61, 1238.
49. Linder, S. W.; Yanik, G. W.; Bobbitt, D. R. *Microchem. J.* **2004**, 76, 105.

50. Goodall, D. M. *Trends Anal. Chem.* **1993**, 12, 177.
51. Finn, M. G. *Chirality* **2002**, 14, 534.
52. Bounoshita, M.; Hibi, K.; Nakamura, H. *Analytical Sciences* **1993**, 9, 425.
53. Yamamoto, A.; Matsunaga, A.; Hayakawa, K.; Miyazaki, M.; Nishimura, M. *J. Chromatogr. A*. **1996**, 727, 55.
54. Yamamoto, A.; Matsunaga, A.; Mizukami, E.; Hayakawa, K.; Miyazaki, M. *J. Chromatogr. A*. **1994**, 667, 85.
55. Yamamoto, A.; Matsunaga, A.; Hayakawa, K.; Mizukami, E.; Miyazaki, M. *Analytical Sciences* **1991**, 7, 719.
56. Hamasaki, K.; Kato, K.; Watanabe, T.; Yoshimura, Y.; Nakazawa, H.; Yamamoto, A.; Matsunaga, A. *J. Pharm. Biomed. Anal.* **1998**, 16, 1275.